PHYSICAL REVIEW C VOLUME 27, NUMBER 5 MAY 1983

Microscopic formalism for intermediate energy transfer reactions: Application to the (p,d) and (d,p) reactions

L. D. Ludeking
Physics Department, Indiana University, Bloomington, Indiana 47401
and Ames Laboratory, United States Department of Energy and Department of Physics, Iowa State University, Ames, Iowa 50011

J. P. Vary
Ames Laboratory, United States Department of Energy and Department of Physics, Iowa State University, Ames, Iowa 50011
(Received 7 January 1983)

Using a multiple scattering framework we construct a variant of the usual distorted-wave Born approximation transition matrix for stripping and pickup reactions. An alternative to the local energy approximation is derived which in the appropriate limit gives the commonly used zero range approximation for (p,d) and (d,p) reactions. Model calculations are developed in an eikonal framework and an examination of the sensitivity and energy dependence of the nuclear response function is made, using the $^{12}C(p,d)^{11}C(\frac{3}{2}^-$, g.s.) process.

[NUCLEAR REACTIONS $(p,d),(d,p)$, intermediate energy, multiple scattering formalism with direct treatment of realistic nucleon-nucleon potential.]

I. INTRODUCTION

As nuclear reactions are studied at higher energies it has become apparent that theories developed for low-energy applications are increasingly taxed to yield results for comparison with data. For direct nuclear reactions such as (p,d), (p,t), (d,t), etc., there is the additional concern that target and projectile correlations[1] play an increasingly important role as the momentum transfer increases at higher bombarding energies. We address the direct reaction problem through a multiple scattering approach which incorporates *directly* a number of important physical mechanisms which appear as corrections to the standard DWBA formalism. The primary advantage of our formulation rests in convenience for high-energy applications. In fact, we imagine that an "improved" DWBA such as a coupled-channel Born approximation (CCBA) with optical potentials including nucleon-nucleon correlation effects could be developed which would be equivalent to our approach.

The general problem of nucleus-nucleus interactions at intermediate energies may be formulated in a variety of ways even within a multiple scattering framework.[2–18] We examine one path for the (p,d) example that begins with the full transfer amplitude and introduce ingredients from a multiple scattering theory that renders a calculable form. A significant effort is devoted to developing a systematic microscopic scheme and illustrative examples are provided. Approximations reminiscent of those used in some DWBA studies such as zero range[19,20] and no recoil are possible and simplify the theory accordingly. We provide calculations with and without approximations to demonstrate their importance. Similarly, we illustrate the role of target correlations at higher energies. For simplicity all (p,d) reaction calculations are performed for a ^{12}C target.

The organization of our paper is as follows: Section II presents the two-potential formula[21] for the transition amplitude suitable for transfer of a cluster between two other clusters. Here we emphasize the many-body nature of these reactions and obtain specific expressions for the (p,d) example. We present a general description of initial and final state wave functions. Section III continues the discussion of the specific (p,d) and (d,p) example with a general treatment of the deuteron vertex function.[22] Section IV details the approximations specific to this application of our approach. Sensitivity studies are presented as well for the $^{12}C(p,d)^{11}C$ example at 700 MeV. In Sec. V we present our conclusions and outlook.

 ©1983 The American Physical Society

II. DIRECT REACTION AMPLITUDE

In order to delineate our approach and introduce our notation we briefly review the two-potential[21] form of the direct reaction transition amplitude. In Appendix A, a number of operator identities are developed which are of general utility and which facilitate the construction of the two-potential amplitude given here in Sec. II A. Some brief comments on the properties of these identities are made. Section II B is concerned with the wave functions and the nucleon-nucleon wave operators.

A. Two potential form of the transition matrix

The conventional form of the T matrix for the transition from an initial channel (i) and state (α) to a final channel (f) and state (β), has two equivalent on-shell expressions,

$$T(i_\alpha \to f_\beta) = \langle \Psi_f^{(-)}(\beta) \mid V^i \mid \phi_i(\alpha) \rangle \tag{2.1}$$

and

$$T(i_\alpha \to f_\beta) = \langle \phi_f(\beta) \mid V^f \mid \Psi_i^{(+)}(\alpha) \rangle \ . \tag{2.2}$$

The total Hamiltonian H is written as

$$H = h_i + V^i = h_f + V^f \ .$$

Here H, whose scattering solutions are $\mid \Psi_{i,f}^{(\pm)}(\alpha) \rangle$ and Green's function is G, describes the exact many body nature of the system, whereas h_i and h_f represent incident and exit channel Hamiltonians for two noninteracting clusters. Thus V^i and V^f are the cluster interactions in the specified channel.

Consider the action of an entrance channel perturbation (denoted by U^i) upon the eigenket $\mid \phi_i(\alpha) \rangle$. From the identity Eq. (A11) of Appendix A, it is evident that

$$\mid \phi_i(\alpha) \rangle = g_i(g_i^{-1} - U^i) \mid \chi_i^{(+)}(\alpha) \rangle \ , \tag{2.3}$$

and from Eq. (A10) it follows that

$$\langle \Psi_f^{(-)}(\beta) \mid = \langle \phi_f(\beta) \mid g_f^{-1} G \ . \tag{2.4}$$

Applying Eqs. (2.3) and (2.4) to Eq. (2.1), we obtain for the transition matrix element the expression

$$T(i_\alpha \to f_\beta) = \langle \phi_f(\beta) \mid g_f^{-1} G [V^i][g_i(g_i^{-1} - U^i)] \mid \chi_i^{(+)}(\alpha) \rangle \ . \tag{2.5}$$

The resolvent identity Eq. (A4) applied to G and g_i leads to

$$G = g_i + g_i V^i G = g_i + G V^i g_i \ . \tag{2.6}$$

Thus

$$g_i V^i G = G V^i g_i \ , \tag{2.7}$$

and Eq. (2.5) becomes

$$T(i_\alpha \to f_\beta) = \langle \phi_f(\beta) \mid g_f^{-1} g_i V^i G (g_i^{-1} - U^i) \mid \chi_i^{(+)}(\alpha) \rangle \ . \tag{2.8}$$

From the resolvent inverse Eq. (A5), note that G^{-1} is $g_i^{-1} - V^i$ and this implies that

$$T(i_\alpha \to f_\beta) = \langle \phi_f(\beta) \mid g_f^{-1} g_i V^i G (G^{-1} + V^i - U^i) \mid \chi_i^{(+)}(\alpha) \rangle \tag{2.9}$$

$$= \langle \phi_f(\beta) \mid g_f^{-1} g_i V^i \mid \chi_i^{(+)}(\alpha) \rangle + \langle \phi_f(\beta) \mid g_f^{-1} g_i V^i G (V^i - U^i) \mid \chi_i^{(+)}(\alpha) \rangle \ . \tag{2.10}$$

Applying Eq. (2.6) this becomes

$$T(i_\alpha \to f_\beta) = \langle \phi_f(\beta) \mid g_f^{-1} g_i V^i \mid \chi_i^{(+)}(\alpha) \rangle + \langle \phi_f(\beta) \mid g_f^{-1} (G - g_i)(V^i - U^i) \mid \chi_i^{(+)}(\alpha) \rangle$$

$$= \langle \phi_f(\beta) \mid g_f^{-1} G (V^i - U^i) \mid \chi_i^{(+)}(\alpha) \rangle + \langle \phi_f(\beta) \mid g_f^{-1} g_i U^i \mid \chi_i^{(+)}(\alpha) \rangle \ , \tag{2.11}$$

or equivalently

$$T(i_\alpha \to f_\beta) = \langle \Psi_f^{(-)}(\beta) \mid (V^i - U^i) \mid \chi_i^{(+)}(\alpha) \rangle + \langle \phi_f(\beta) \mid g_f^{-1} g_i U^i \mid \chi_i^{(+)}(\alpha) \rangle \ . \tag{2.12}$$

Equation (2.12) is the form alluded to in the literature as the two-potential formula.[21] If the interaction U^i is an optical potential connecting only elastic and inelastic scattered states of the incident channel, then Lippmann's identity[23] obtains and the second term is zero. However, for a general many-body scattering interaction this may not be the case and this term can connect breakup states of the incident channel with the two-cluster exit channel. Nevertheless, the frequently made assumptions in distorted wave approximations actually force the second term to zero. Insofar as these assumptions are valid the first term of Eq. (2.12) is dominant.

Suppose we consider that class of direct reactions described as two-cluster rearrangement collisions. Schematically such processes may be represented by

$$A+(BC)\rightarrow(AC)+B\ , \tag{2.13}$$

where (BC) and (AC) are bound states of the clusters B, C and A, C, respectively.

The Hamiltonians for A, B, and C are h_A, h_B, and h_C. The total noninteracting Hamiltonian h_0 is defined

$$h_0=h_A+h_B+h_C\ . \tag{2.14}$$

The interactions which form the bound states (BC) and (AC) are V_{BC} and V_{AC}. The total interaction between the clusters A, B, and C is

$$V^0=V_{AB}+V_{BC}+V_{AC}\ . \tag{2.15}$$

The channel Hamiltonians for the reaction in Eq. (2.13) are

$$h_i=h_0+V_{BC}=h_0+V_i \tag{2.16}$$

and

$$h_f=h_0+V_{AC}=h_0+V_f\ . \tag{2.17}$$

The channel interactions become

$$V^i=V^0-V_i=V_{AB}+V_{AC} \tag{2.18}$$

and

$$V^f=V^0-V_f=V_{AB}+V_{BC}\ . \tag{2.19}$$

The total Hamiltonian H may be described as

$$H=h_a+V^a,\ \ a=(0,\ i,\ \text{or}\ f)\ . \tag{2.20}$$

The corresponding propagators g_a, G are constructed as before.

Consider the two-potential formula letting $U^i=V_{AB}$; this becomes

$$T(i_\alpha\rightarrow f_\beta)=\langle\Psi_f^{(-)}(\beta)\,|\,V_{AC}\,|\,\chi_i^{(+)}(\alpha)\rangle + \langle\phi_f(\beta)\,|\,g_f{}^{-1}g_iV_{AB}\,|\,\chi_i^{(+)}(\alpha)\rangle\ . \tag{2.21}$$

The contributions from the second term of Eq. (2.21) depend upon the exact nature of the rearrangement channel and energy regime of interest.

Consider specifically the $p+A\rightarrow d+B$ or $A(p,d)B$ rearrangement process and the contribution of the first term in Eq. (2.21) to the transition amplitude. We write

$$T(i_\alpha\rightarrow f_\beta)=\langle\Psi_f^{(-)}(\beta)\,|\,V_{pn}\,|\,\chi_i^{(+)}(\alpha)\rangle\ . \tag{2.22}$$

Physically $|\chi_i^{(+)}(\alpha)\rangle$ denotes a distorted wave generated from the unperturbed initial state $|\phi_i(\alpha)\rangle$ through the perturbation of the potential V_{pB}.

$$|\chi_i^{(+)}(\alpha)\rangle=|\Phi_i(\alpha)\rangle+g_i^{(+)}V_{pB}\,|\,\chi_i^{(+)}(\alpha)\rangle \tag{2.23}$$

$$=[1+(E_i-i\eta-h_i-V_{pB})^{-1}V_{pB}]\,|\,\Phi_i(\alpha)\rangle=\overline{\Omega}_i^{(+)}\,|\,\phi_i(\alpha)\rangle\ . \tag{2.24}$$

The final scattering state $\langle\Psi_f^{(-)}(\beta)\,|$ can be obtained from Eq. (2.4) after some manipulations to be

$$\langle\Psi_f^{(-)}(\beta)\,|=\langle\phi_f(\beta)\,|\left[1+V_{dB}\frac{1}{E-i\eta-h_f-V_{dB}}\right]=\langle\phi_f(\beta)\,|\,\Omega_f^{(-)}\ . \tag{2.25}$$

Thus

$$T(i_\alpha\rightarrow f_\beta)=\langle\phi_f(\beta)\,|\,\Omega_f^{(-)}V_{pn}\overline{\Omega}_i^{(+)}\,|\,\phi_i(\alpha)\rangle\ . \tag{2.26}$$

B. Wave function treatment

The wave functions Φ_i and Φ_f represent channel solutions of the entrance and exit channel eigenequations. As bombarding energy increases we expect to be able to neglect antisymmetrization between the two clusters in both incoming and outgoing states. Therefore, we take the unsymmetrized wave functions as a product of plane waves for the two clusters with the intrinsic wave functions for each. That is,

$$\Phi_i=\left[\frac{1}{2\pi}\right]^3 e^{i\vec{k}_p\cdot\vec{r}_p+i\vec{k}_A\cdot\vec{R}_A}X^p_{S_p\mu_p}\sum_{L_Am_A,S_A\mu_A}\langle J_AM_A\,|\,L_Am_AS_A\mu_A\rangle U^A_{L_Am_A}X^A_{S_A\mu_A} \tag{2.27}$$

and

$$\Phi_f=\left[\frac{1}{2\pi}\right]^3 e^{i\vec{k}_d\cdot\vec{r}_d+i\vec{k}_B\cdot\vec{R}_B}\sum_{L_Bm_B,S_B\mu_B}\langle J_BM_B\,|\,L_Bm_BS_B\mu_B\rangle U^B_{L_Bm_B}X^B_{S_B\mu_B} \times\sum_{L_dm_d,S_d\mu_d}\langle J_dM_d\,|\,L_dm_dS_d\mu_d\rangle U^d_{L_dm_d}X^d_{S_d\mu_d}\ . \tag{2.28}$$

Here X is the spin function, U is the space wave function, and $\langle\ |\ \rangle$ is the conventional Clebsch-Gordan coupling constant.

The wave functions $\Psi_f^{(-)}(\beta)$ and $\chi_i^{(+)}(\alpha)$ are those evolved from $\Phi_f(\beta)$ and $\Phi_i(\alpha)$ according to Eqs. (2.25) and (2.24), respectively, and can be written

$$\chi_i^{(+)}=e^{i\phi_{pB}^{+}(a)}\phi_i(\alpha) \tag{2.29a}$$

and

$$\Psi_f^{(-)}=e^{+i\phi_{dB}^{-}(a)}\Phi_f(\alpha)\ ,$$
$$a=\{(\vec{r},\vec{\sigma},\vec{\tau})_i\}\ ,\quad i\epsilon(p,n,1,2,\ldots,B)\ . \tag{2.29b}$$

Alternatively, we could interpret these forms in the momentum representation. The operators $\phi_{pB}^{+}(a)$ and $\phi_{dB}^{-}(a)$ defined by

$$e^{i\phi_{pB}^{+}(a)}=1+[E_i-i\eta-h_i-V_{pB}]^{-1}V_{pB}\ , \tag{2.30a}$$

$$e^{-i\phi_{dB}^{-}(a)}=1+[E_f+i\eta-h_f-V_{dB}]^{-1}V_{dB}\ , \tag{2.30b}$$

generate the many-body distorted waves.

In order to simplify the problem further, we assume that $[V_{pn},\exp(i\phi_{dB}^{-}(a))]=0$. This amounts to approximating some of the intermediate excitations of the deuteron and target. Since all possible channels of the scattering system are contained in $\langle\Psi_f^{(-)}|$, we have replaced these couplings by approximate global effects. At higher energies and higher momentum transfer this should be a reasonable assumption.

The amplitude for the neutron pickup reaction is written as $T_{pd}=T(J_AM_AS_p\mu_p\,|\,J_BM_BJ_dM_d)$,

$$T=\sum_{\substack{\text{sum over}\\ \text{repeated}\\ \text{indices}}}\langle J_AM_A\,|\,L_Am_AS_A\mu_A\rangle\langle J_BM_B\,|\,L_Bm_BS_B\mu_B\rangle\langle J_dM_d\,|\,L_dm_dS_d\mu_d\rangle$$
$$\times\langle S_d\mu_dS_B\mu_B\,|\,T(L_Am_A;L_Bm_BL_dm_d)\,|\,S_A\mu_AS_p\mu_p\rangle\ , \tag{2.31}$$

where the quantity $T(L_Am_A;L_Bm_BL_dm_d)$ is defined by

$$T(L_Am_A;L_Bm_BL_dm_d)\equiv\left[\frac{1}{2\pi}\right]^3\int d^3r_p\,d^3r_n\,e^{i\vec{Q}_p\cdot\vec{r}_p+i\vec{Q}_n\cdot\vec{r}_n}d_{L_dm_d}(\vec{r}_p-\vec{r}_n)N_{L_Am_A}^{L_Bm_B}(\vec{r}_p,\vec{r}_n) \tag{2.32}$$

when we neglect spin-flip contributions, and, where

$$\vec{Q}_p=\vec{k}_p-\tfrac{1}{2}\vec{k}_d\ , \tag{2.33}$$

$$\vec{Q}_n=-\tfrac{1}{2}\vec{k}_d-\frac{1}{A}\vec{k}_p\ . \tag{2.34}$$

In Eq. (2.32) the quantities $d_{L_dm_d}$ are the deuteron vertex functions defined in Appendix B and contain the information about the deuteron wave function and the proton-neutron interaction. For convenience, we present in Tables I and II a simple expansion for the main ingredients of the vertex functions. Consult Appendix B for necessary definitions. The function N contains the neutron overlap wave function between the incident A-particle nucleus and the residual B-particle nucleus as well as the distortion factors arising from the interaction of the B spectators in both the entrance and exit channels. In terms of the wave function U^B and U^A, this function is

$$N_{L_Am_A}^{L_Bm_B}(\vec{r}_p,\vec{r}_n)=\int d^3r_1\cdots d^3r_B\,U_{L_Bm_B}^{B}(\vec{r}_1,\vec{r}_2\cdots\vec{r}_B)W(\vec{r}_p,\vec{r}_n,\vec{r}_1,\vec{r}_2\cdots\vec{r}_B)U_{L_Am_A}^{A}(\vec{r}_n,\vec{r}_1,\vec{r}_2\cdots\vec{r}_B) \tag{2.35}$$

and W, the distortion operator, is

$$W(\vec{r}_p,\vec{r}_n\cdots\vec{r}_B)=\exp[i\phi_{dB}^{-}(a)]\times\exp[i\phi_{pB}^{+}(a)]\ . \tag{2.36}$$

The more conventional DWBA approach to (p,d) reactions may be obtained by recognizing that the operator W plays the same role as do the optical potentials typically used for generating the partial

TABLE I. Gaussian fit coefficients of deuteron D-state vertex function generated from the Reid soft core potential.

Form: $U_D^{\text{eff}}(r)=r^3\sum_{j=1}^{M} C_j^D \exp(-\alpha_j^D r^2)$.

$M=25$. $E+n$ denotes 10^{+n}.

j	C_j^D	α_j^D
1	0.202401389E +05	0.6684000E +01
2	−0.109807802E +05	0.4856000E +01
3	−0.928291412E +05	0.2025500E +02
4	−0.508055445E +01	0.6063700E −01
5	0.245980712E +05	0.2668785E +02
6	0.755105860E +05	0.1846687E +02
7	−0.150645649E +05	0.8345700E +01
8	0.383771269E +04	0.3812730E +01
9	−0.743267863E +03	0.2346205E +01
10	0.495399774E +01	0.6438500E +00
11	−0.361225251E +02	0.8784360E +00
12	−0.292575389E +01	0.4166280E +00
13	0.744244322E +00	0.2770020E +00
14	−0.835869562E +00	0.2190330E +00
15	0.591109352E +00	0.1690240E +00
16	−0.410052537E +00	0.1398840E +00
17	0.397091629E +01	0.5520000E −01
18	0.295198160E +00	0.9918500E −01
19	0.215205079E +01	0.7357200E −01
20	0.452251513E +01	0.6751000E −01
21	0.137762997E −01	0.3280000E −01
22	0.128568372E +00	0.4050000E −01
23	−0.123987356E −02	0.2940000E −01
24	−0.152474263E +01	0.5124000E −01
25	−0.630612858E −01	0.3650000E −01

TABLE II. Gaussian fit coefficients of deuteron S-state vertex function generated from the Reid soft core potential.

Form: $U_S^{\text{eff}}=r\sum_{j=1}^{M} C_j^S \exp(-\alpha_j^S r^2)$.

$M=25$. $E+n$ denotes 10^{+n}.

j	C_j^S	α_i^S
1	0.610843938E +04	0.6684000E +01
2	−0.493661552E +04	0.4856000E +01
3	−0.510669294E +03	0.2025500E +02
4	−0.464254205E +02	0.6063700E −01
5	−0.836547450E +02	0.2668700E +02
6	0.324647985E +03	0.1846687E +02
7	−0.352815065E +04	0.8324570E +01
8	0.331105825E +04	0.3812730E +01
9	−0.607184429E +03	0.2346205E +01
10	−0.755349402E +02	0.8784360E +00
11	0.967643543E +01	0.6438500E +00
12	−0.702864658E +01	0.4166280E +00
13	0.351786070E +01	0.2770020E +00
14	−0.447701126E +01	0.2190330E +00
15	0.401673683E +01	0.1690240E +00
16	−0.309415610E +01	0.1398840E +00
17	0.365288268E +02	0.5520000E −01
18	0.250157011E +01	0.9918500E −01
19	−0.193038190E +02	0.7357200E −01
20	0.409315843E +02	0.6751000E −01
21	0.129979375E +00	0.3280000E −01
22	0.120128136E +01	0.4050000E −01
23	−0.117946403E −01	0.2940000E −01
24	−0.140895297E +02	0.5124000E −01
25	−0.591960040E +00	0.3650000E −01

wave expansions for the scattering of protons and deuterons from a target.

By inserting a complete set of wave functions of the residual target B, the function N of Eq. (2.35) may be written as the product of the pickup neutron wave function $U(r)$ and the integrated distortion factor $F(\vec{r}_p,\vec{r}_n)$. That is,

$$N_{L_A m_A}^{L_B m_B}(\vec{r}_p,\vec{r}_n)=\sum_{\lambda_B \nu_B} U_{L_A m_A}^{\lambda_B \nu_B}(\vec{r}_n) F_{\lambda_B \nu_B}^{L_B m_B}(\vec{r}_p,\vec{r}_n) , \tag{2.37}$$

$$U_{L_A m_A}^{\lambda_B \nu_B}(\vec{r}_n)=\int d^3r_1 \cdots d^3r_B U_{\lambda_B \nu_B}^{B*} U_{L_A m_A}^{A} , \tag{2.38}$$

and

$$F_{\lambda_B \nu_B}^{L_B m_B}(\vec{r}_p,\vec{r}_n)=\int d^3r_1 \cdots d^3r_B U_{L_B m_B}^{B*} W U_{\lambda_B \nu_B}^{B} . \tag{2.39}$$

From these expressions it is evident how specific multistep processes may be included. Intermediate states may be included in the incident channel as well. We consider a direct nuclear reaction to be one which is dominated by at most a few states coupled significantly to the initial and final states.

III. MODEL FEATURES FOR (p,d) APPLICATION

A. The deuteron vertex function and sensitivities

At low energies (less than ~100 MeV) the traditional approach to calculating the transition amplitude Eq. (2.32) has been to replace the vertex functions $d_{LM}(\vec{r})$ by point vertex functions[24] of the form

$$d_{LM}(\vec{r}_P-\vec{r}_N)\approx d_{LM}^0 \delta(\vec{r}_p-\vec{r}_n) . \tag{3.1}$$

A variety of approaches[25,26] have been used to correct this feature. Studies of corrections to zero

range have typically found significant effects[27] at modes and energies $\lesssim 160$ MeV. Extensive finite range and zero range calculations (notably by the Colorado group)[28] using the standard DWBA at intermediate energies have generally provided limited success in explaining cross sections[29–31] and analyzing powers.[32–34] Although it is common to retain only the S-state vertex at low energies ($\lesssim 40$ MeV), since this term typically dominates the (p,d) reaction, some investigators[35,36] have considered the effect of S and D contributions to the vector and tensor analyzing powers ($\lesssim 10$ MeV). These investigations displayed large sensitivity to the presence of the deuteron D state only in the tensor analyzing powers. In addition, Delic and Robson[35] considered the effect of a finite range treatment on the (d,p) cross sections (8 MeV); they found that the primary result was to change the overall normalization of the resulting cross sections. In order to demonstrate the relative contributions of the S-state and D-state deuteron vertex function, we examine the Fourier transform as it varies with momentum mismatch $\vec{q}$. The Fourier transform of the deuteron vertex function is defined by

$$\tilde{d}_{LM}(\vec{Q})=\int e^{i\vec{Q}\cdot\vec{r}}d_{LM}(\vec{r})d^3r \tag{3.2}$$

or

$$\tilde{d}_{LM}(\vec{Q})=(i)^L Y_{LM}(\hat{Q})D_L(Q)\ , \tag{3.3}$$

where

$$D_L(Q)=4\pi\int_0^\infty r j_L(Qr)U_L^{\rm eff}(r)dr\ . \tag{3.4}$$

The momentum mismatch $\vec{q}=\vec{k}_p-\vec{k}_d/2$ is a function of the incident proton kinetic energy and the mass of the target. Figure 1 plots the vertex function $D_L(q)$ vs q, and the incident kinetic energy against q for forward scattering. As can be seen at low momentum mismatch, the S state dominates, whereas between 1.3 and 3.4 fm^{-1} the D state dominates. At about 500 MeV proton kinetic energy the S-state contribution is virtually zero. The forward cross section for 700 MeV kinetic energy is largely D state, with a significant admixture of S state as well.

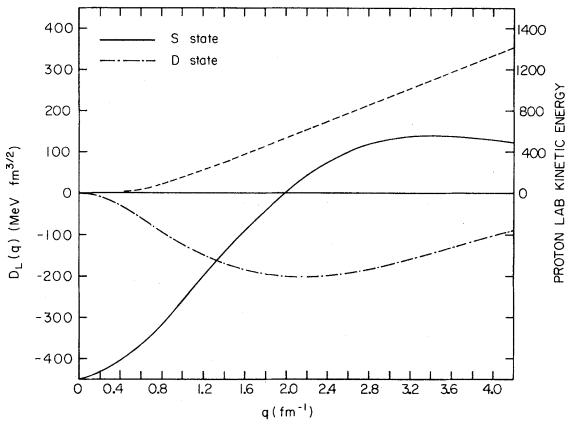

FIG. 1. Momentum dependence of the deuteron vertex functions. The solid (dotted-dashed) curve shows the behavior of the S-state (D-state) deuteron vertex function $D_L(q)$ (calculated from the Reid soft core parametrization) as a function of q (momentum transfer). The dashed curve shows the q value ($q=k_p-\frac{1}{2}k_d$) at 0° for ^{12}C(p,d) as a function of proton laboratory kinetic energy.

In order to address the questions about sensitivities in a systematic fashion, we rewrite Eq. (2.32) for the transition amplitude with the Fourier transforms of the vertex functions. Thus

$$T(L_Am_A;L_Bm_BL_Dm_D)=\left[\frac{1}{2\pi}\right]^6\int d^3k\,\tilde{d}_{L_Dm_D}(\vec{Q}_p-\vec{k})\int d^3r_n d^3r_p e^{i\vec{Q}\cdot\vec{r}_n+i\vec{k}\cdot(\vec{r}_p-\vec{r}_n)}N_{L_Am_A}^{L_Bm_B}(\vec{r}_p,\vec{r}_n) \tag{3.5}$$

and

$$\vec{Q}=\vec{Q}_p+\vec{Q}_n\ . \tag{3.6}$$

The zero-range approximation is obtained by examining the Taylor series expansion of the vertex functions $\tilde{d}_{L_Dm_D}(\vec{Q}_p-\vec{k})$ about $\vec{k}=0$. We write as

$$\tilde{d}_{LM}(\vec{Q}_p-\vec{k})=\sum_{n=0}^{\infty}\frac{(-\vec{k}\cdot\vec{\nabla}_k)^n}{n!}\tilde{d}_{LM}(\vec{k})\,|_{\vec{k}=\vec{Q}_p} \tag{3.7}$$

$$=i^L Y_{LM}(\hat{Q}_p)\sum_{n=0}^{\infty}\frac{(-k\partial/\partial k)^n}{n!}D_L(k)\,|_{k=Q_p}\ . \tag{3.8}$$

Substitution of Eq. (3.7) into Eq. (3.5) yields for the transition amplitude the expression

$$T=\sum_{n=0}^{\infty}T_n\ , \tag{3.9}$$

where the nth term is defined as

$$T_n=\frac{1}{(2\pi)^6}\int d^3k\,d^3r_p d^3r_n\left[\frac{(-\vec{k}\cdot\vec{\nabla}_{Q_p})^n}{n!}\tilde{d}_{L_d m_d}(\vec{Q}_p)\right]e^{i\vec{Q}\cdot\vec{r}_n+i\vec{k}\cdot(\vec{r}_p-\vec{r}_n)}N_{L_A m_A}^{L_B m_B}(\vec{r}_p,\vec{r}_n)\ . \tag{3.10}$$

The $n=0$ zero term is

$$T_0=\frac{1}{(2\pi)^3}\tilde{d}_{L_d m_d}(\vec{Q}_p)\int d^3r\,e^{i\vec{Q}\cdot\vec{r}}N_{L_A m_A}^{L_B m_B}(\vec{r},\vec{r})\ . \tag{3.11}$$

We refer to this term as the zero-range truncation (ZRT). The ZRT has the advantage over the conventional zero-range approximation in that the strength of the vertex constants are specified rather than adjusted from a phenomenological basis. Furthermore, it includes both the S-state and D-state strengths. The general term for arbitrary n may be simplified by repeated use of the divergence theorem and the chain rule for differentiation. Under these manipulations Eq. (3.10) becomes

$$T_n=\frac{1}{(2\pi)^3}\int d^3r_n d^3r_p\,\delta(\vec{r}_p-\vec{r}_n)e^{i\vec{Q}\cdot\vec{r}_n}\frac{(i\vec{\nabla}_{r_p}\cdot\vec{\nabla}_{Q_p})^n}{n!}N_{L_A m_A}^{L_B m_B}(\vec{r}_p,\vec{r}_n)\tilde{d}_{L_d m_d}(\vec{Q}_p)\ . \tag{3.12}$$

A simple examination reveals that Eq. (3.12) reduces to Eq. (3.11) for $n=0$, as it should. From the form of Eq. (3.12) it is clear that unless the series Eq. (3.9) converges very rapidly in the energy regime of interest, the "simplification" introduced [Eq. (3.12)] would not present any advantage over an exact finite range calculation, since the gradient mixing terms may be difficult to evaluate. However, it is evident from Fig. 1 that the vertex functions are slowly varying and smoothly behaved; thus if the matrix elements are evaluated at the momentum transfer of interest, the leading correction term should be T_1.

$$T_1=\left[\frac{1}{2\pi}\right]^3\int d^3r_n d^3r_p\,\delta(\vec{r}_p-\vec{r}_n)e^{i\vec{Q}\cdot\vec{r}_n}(i\vec{\nabla}_{r_p}\cdot\vec{\nabla}_{Q_p})N_{L_A m_A}^{L_B m_B}(\vec{r}_p,\vec{r}_n)\tilde{d}_{L_d m_d}(\vec{Q}_p)\ , \tag{3.13}$$

$$=i\left[\frac{1}{2\pi}\right]^3\int d^3r_n d^3r_p\,\delta(\vec{r}_p-\vec{r}_n)e^{i\vec{Q}\cdot\vec{r}_n}\{\vec{\nabla}_{r_p}N_{L_A M_A}^{L_B M_B}(\vec{r}_p,\vec{r}_n)\}\cdot\{\vec{\nabla}_{Q_p}\tilde{d}_{L_d m_d}(\vec{Q}_p)\}\ . \tag{3.14}$$

B. The distortion function

The evaluation of the distortion factor F which accommodates the perturbations of the nuclear media on the incident and exiting waves depends in detail upon the distortion function W, Eq. (2.36). As can be seen from Eqs. (2.30a), (2.30b), and (2.36) this ultimately requires some knowledge of the distortion operators ϕ_{pB}^{+} and ϕ_{dB}^{-}.

For intermediate energies the eikonal (or high energy approximation[37–39]) has been used with some success in elastic and inelastic scattering.[2,40–42] Tekou[43] has applied it to a formulation of the pick-up reaction, although his approach is considerably different from ours in emphasis and detail.

In an eikonal framework these operators are defined in terms of the nucleon-nucleon eikonal phase shift functions $\chi^{\pm}$ by the expressions

$$\phi_{pB}^{+}=\sum_{j\in B}\chi_{pj}^{+} \tag{3.15}$$

and

$$\phi_{dB}^{-}=\sum_{j\in B}[\chi_{pj}^{-}+\chi_{nj}^{-}]\ . \tag{3.16}$$

The eikonal phase shifts $\chi^{\pm}$ are defined by

$$\chi_{jl}^{+}(\vec{r})=-\frac{1}{\hbar v_{jl}}\int_{-\infty}^{z}V_{jl}(\vec{r})dz' \tag{3.17}$$

and

$$\chi_{jl}^{-}(\vec{r})=-\frac{1}{\hbar v_{jl}}\int_{z}^{\infty}V_{jl}(\vec{r})dz'\ , \tag{3.18}$$

where v_{jl} is the relative velocity of nucleons j and l and $V_{jl}(\vec{r})$ is the nucleon-nucleon interaction. Furthermore, nucleon-nucleon distortion functions $w^{\pm}$ are defined by

$$w_{jl}^{\pm}\equiv 1-\exp(i\chi_{jl}^{\pm})\ . \tag{3.19}$$

The phase shift functions are then related to the elementary, nucleon-nucleon scattering amplitude $A(\vec{q})$ through the integral expression

$$A(\vec{q})=-\mu/2\pi\hbar^2\int d\tau e^{i\vec{q}\cdot\vec{r}}Ve^{+i\chi^{+}}\ , \tag{3.20}$$

where μ is the reduced nucleon-nucleon mass. Note that in expression (3.20), the spin and isospin dependence of the potential and scattering amplitude $A(\vec{q})$ is left implicit. For our model calculations we

assume $A(\vec{q})$ to be the spin-isospin averaged elastic scattering amplitude. In the remaining development we explicitly include only the $\vec{r}$ dependence.

In order to demonstrate the connection between the scattering amplitude $A(\vec{q})$ and the distortion functions $w^{\pm}(\vec{r})$, note that Eqs. (3.19) can be written in integral form as

$$w^{+}(\vec{r})=i/\hbar v\int_{-\infty}^{z}V(\vec{b},z')e^{i\chi^{+}(\vec{b},z')}dz' \quad (3.21)$$

and

$$w^{-}(\vec{r})=i/\hbar v\int_{z}^{\infty}V(\vec{b},z')e^{i\chi^{-}(\vec{b},z')}dz' . \quad (3.22)$$

Taking the Fourier transform of $A(\vec{q})$ then yields for $w^{\pm}(\vec{r})$ the expressions

$$w^{+}(\vec{r})=\frac{1}{(2\pi)^2 ik}\int d^3q\,A(\vec{q}_t,q_z)e^{-i\vec{q}_t\cdot\vec{b}}\times\int_{-\infty}^{z}e^{-iq_z\cdot z'}dz' \quad (3.23)$$

and

$$w^{-}(\vec{r})=\frac{1}{(2\pi)^2 ik}\int d^3q\,A(\vec{q}_t,q_z)e^{-i\vec{q}_t\cdot\vec{b}}\times\int_{z}^{\infty}e^{-iq_z\cdot z'}dz' , \quad (3.24)$$

where $\vec{q}_t$ and q_z are the transverse and longitudinal momentum transfers, respectively, and k is the relative momentum.

Expanding the amplitude $A(\vec{q})$ in a Taylor series about $q_z=0$, we obtain the expression

$$A(\vec{q})=\sum_{n=0}^{\infty}\frac{(q_z)^n}{n!}A^{(n)}(\vec{q}_t,0) , \quad (3.25)$$

where

$$A^{(n)}(\vec{q}_t,0)=(\partial/\partial q_z)^n A(q)\,|_{q_z=0} . \quad (3.26)$$

Substitution of Eq. (3.25) into Eqs. (3.23) and (3.24) yields the relations

$$w^{\pm}(r)=\frac{1}{2\pi ik}\sum_{n=0}\frac{(i)^n}{n!}\Phi_n^{\pm}(z)\bar{A}^{(n)}(b) \quad (3.27)$$

$$=\sum_{n=0}w_n^{\pm}(r) , \quad (3.28)$$

where

$$\Phi_n^{+}(z)=\int_{-\infty}^{z}\delta^{(n)}(z')dz' , \quad (3.29)$$

$$\Phi_n^{-}(z)=\int_{z}^{\infty}\delta^{(n)}(z')dz' , \quad (3.30)$$

and

$$\bar{A}^{(n)}(\vec{b})=\int d^2q_t A^{(n)}(\vec{q}_t,0)e^{-i\vec{q}_t\cdot\vec{b}} . \quad (3.31)$$

Here $\delta(z)$ is the Dirac delta function, and the derivatives $\delta^{(n)}(z)$ are defined by

$$\delta^{(n)}(z)=(d/dz)^n\delta(z) . \quad (3.32)$$

The properties of the functions $\Phi_n^{\pm}(z)$ are summarized below.

$$\Phi_0^{+}(z)=\theta^{+}(z)=\begin{cases}1, & z>0\\ \frac{1}{2}, & z=0\\ 0, & z<0\end{cases} , \quad (3.33a)$$

$$\Phi_0^{-}(z)=\theta^{-}(z)=\begin{cases}0, & z>0\\ \frac{1}{2}, & z=0\\ 1, & z<0\end{cases} , \quad (3.33b)$$

$$\Phi_0^{+}(z)+\Phi_0^{-}(z)=1 , \quad (3.34)$$

$$\Phi_n^{-}(z)=(-)^n\Phi_n^{+}(-z);\quad n=0,1,2,\ldots . \quad (3.35)$$

Equation (3.35) is the reflection identity for $\Phi_n^{\pm}$.

Consider a typical representation of the spin-isospin averaged nucleon-nucleon scattering amplitude to be the parametrization

$$A(q)=\frac{ik}{4\pi}\sigma^{\text{tot}}(1-i\alpha)e^{-\beta^2q^2/4} . \quad (3.36)$$

In Eq. (3.36), k is the relative momentum, σ^{tot} is total nucleon-nucleon cross section at the interaction energy, α is the ratio of real to imaginary strengths of the forward elastic amplitude, and β is a measure of the nucleon-nucleon range. Although, in general, k, σ^{tot}, α, and β are different for the incoming and outgoing waves, we average over these variations as well.

The parametrization Eq. (3.36) when inserted in Eqs. (3.27) and (3.28) for the $w_n^{\pm}(\vec{r})$ yields

$$w_n^{\pm}(r)=\frac{(+i)^n}{n!}\gamma(b)\Phi_n^{\pm}(z)(-\beta/2)^n H_n(0) , \quad (3.37)$$

where

$$\gamma(b)=\frac{1}{2\pi\beta^2}\sigma^{\text{tot}}(1-i\alpha)e^{-b^2/\beta^2} , \quad (3.38)$$

and the $H_n(0)$ are the Hermite polynomials evaluated at zero. The $H_n(0)$ satisfy the recurrence equation

$$H_{n+2}(0)=(-2)(n+1)H_n(0) . \quad (3.39)$$

The initial values $H_0=1$ and $H_1=0$ then imply that in $w^{\pm}(\vec{r})$ all $n=$odd integer terms vanish, and furthermore that

$$w_0^{\pm}(\vec{r})=\Gamma(b)\theta^{\pm}(z) , \quad (3.40)$$

$$w_n^{\pm}(\vec{r})=\pm\gamma(b)\delta^{(n-1)}(z)\frac{(\beta/\sqrt{2})^n}{n!}[(n-1)!!] \tag{3.41}$$

$n=2,4,6,\ldots$.

Define now the quantities $\zeta^{\pm}(z)$, such that

$$w^{\pm}(\vec{r})=\gamma(b)\zeta^{\pm}(z) . \tag{3.42}$$

We immediately write for $\zeta^{\pm}(z)$ the expression

$$\zeta^{\pm}=\theta^{\pm}(z) \pm \sum_{n=2\ (\text{even integers})} \delta^{(n-1)}(z)(\beta/\sqrt{2})^n\frac{(n-1)!!}{n!} \tag{3.43}$$

The nucleon-nucleon distortion function $w^{\pm}(\vec{r})$ is usually truncated at the first term. The effect of such a truncation on a simple radial density function $\rho(r)$ is investigated in the next section. The familiar Glauber multiple scattering approximations[12,13,40] are the result of such a truncation in the application of the eikonal procedure to elastic and inelastic scattering.

C. Convergence of the nucleon-nucleon distortion functions

The nucleon-nucleon distortion functions $w^{\pm}(\vec{r})$ appear only in integrals over nuclear density functions. Consider a model density function $\rho(r)$, which is parametrized by a normalized Gaussian distribution of the form

$$\rho(r)=\frac{1}{R_0{}^3\pi^{3/2}}e^{-r^2/R_0{}^2} . \tag{3.44}$$

Here the rms radius is $\sqrt{3/2}R_0$ and R_0 is a measure of the nuclear size.

Define a function $T(\vec{r})$ by

$$T^+(\vec{r})\equiv\int d^3r'\rho(r')w^+(\vec{r}-\vec{r}') , \tag{3.45}$$

or alternatively by

$$T^+(\vec{r})=\sum_{n=0}^{\infty}T_n^+(\vec{r}) , \tag{3.46}$$

where by using Eq. (3.28), the $T_n^+(\vec{r})$ can be shown to equal

$$T_n^+(\vec{r})=\int d^3r'\rho(r')w_n^+(\vec{r}-\vec{r}') . \tag{3.47}$$

Substitution of Eqs. (3.40) and (3.41) into Eq. (3.47) then gives

$$T_0^+(\vec{r})=t(\vec{b})\begin{cases}1-\Gamma(\frac{1}{2},z^2/R_0{}^2)/2\pi^{1/2}, & z>0\\ \Gamma(\frac{1}{2},a^2/R_0{}^2)/2\pi^{1/2}, & z<0\end{cases} \tag{3.48}$$

and

$$T_n^+(\vec{r})=t(\vec{b})\left\{-\frac{(n-1)!!}{n!}(\beta/\sqrt{2}R_0)^n h_{n-1}(z/R_0)\right\} , \tag{3.49}$$

for $n=2,4,6,\ldots$, and

$$T_n^+(\vec{r})=0 , \quad \text{for } n=1,3,5,\ldots; \tag{3.50}$$

the function $\Gamma(\frac{1}{2},x^2)$ is the incomplete gamma function defined by the equation

$$\Gamma(\tfrac{1}{2},x_0{}^2)=2\int_{x_0}^{\infty}e^{-t^2}dt, \quad x_0\geq 0 , \tag{3.51}$$

and the transverse function $t(\vec{b})$ is defined by

$$t(b)=\sigma^{\text{tot}}[(1-i\alpha)/2\pi(\beta^2-R_0{}^2)]\exp(-b^2/(\beta^2+R_0{}^2)) . \tag{3.52}$$

The functions $h_n(x)$ are the Gaussian weighted Hermite polynomials

$$h_n(x)=H_n(x)e^{-x^2} , \tag{3.53}$$

and satisfy the recursion equation

$$h_{n+1}(x)=2xh_n(x)-2nh_{n-1}(x); \tag{3.54}$$

the initial values of $H_n(x)$ are $H_0=1$ and $H_1=2x$.

From the results of Eqs. (3.48)–(3.50) it is evident that in this model, $T^+(\vec{r})$ is factorable into a function of z, and the function $t(b)$ of the transverse coordinate. We write

$$T^+(\vec{r})=t(b)\zeta^+(z) . \tag{3.55}$$

The function $\zeta^+(z)$ is defined for $z>0$ as

$$\zeta^+(z)=1-\Gamma(\tfrac{1}{2},z^2/R_0{}^2) -\sum_{n=1}^{\infty}\frac{(2n-1)!!}{(2n)!}\left[\frac{\beta^2}{2R_0{}^2}\right]^n \times h_{2n-1}(z/R_0) , \tag{3.56a}$$

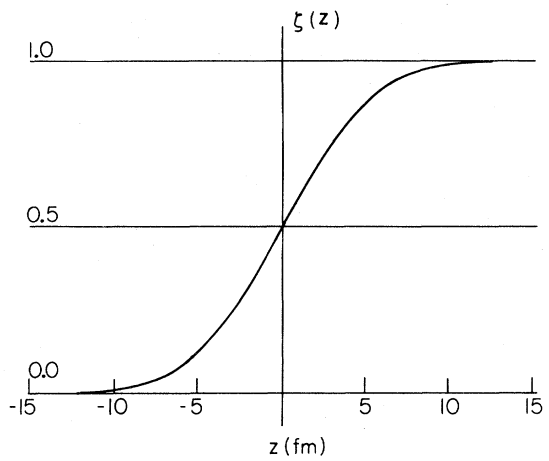

FIG. 2. The z dependence of the transparency function $\zeta(z)$ is displayed for parameters $\beta=1.4$ fm and $R_0=6.0$ fm.

and for $z<0$ as

$$\zeta^+(z)=\Gamma(\tfrac{1}{2},z^2/R_0{}^2) - \sum_{n=1}^{\infty}\frac{(2n-1)!!}{(2n)!}\left[\frac{\beta^2}{2R_0{}^2}\right]^n \times h_{2n-1}(z/R_0)\,. \tag{3.56b}$$

A careful examination shows that the function $(\zeta^+(z)-\frac{1}{2})$ is antisymmetric about $z=0$. Figure 2 shows the characteristic behavior of $\zeta^+(z)$ for $\beta=1.4$ and $R_0=6.0$.

We investigate the convergence of $\zeta^+(z)$ by examining the asymptotic behavior of the nth term of the series for fixed $x=z/R_0$,

$$S_n=(\beta^2/2R_0{}^2)^n\frac{(2n-1)!!}{(2n)!}h_{2n-1}(x)\,. \tag{3.57}$$

The asymptotic behavior of $h_n(x)$ (Ref. 44) is

$$h_n(x)\simeq\left[\frac{x}{\pi}\right]^{1/2}2^n e^{-x^2/2}\Gamma\left[\frac{n+1}{2}\right] \times\cos[x(1+2n)^{1/2}-n\pi/2] \times[1+\mathcal{O}(|n+\tfrac{1}{2}|^{-1/2})]\,. \tag{3.58}$$

Substitution of Eq. (3.58) into Eq. (3.57) yields after simplification

$$S_n\simeq\frac{(\beta^2/R_0{}^2)^n}{n}\left[\frac{x}{\pi}\right]^{1/2}e^{-x^2/2}(-)^n \times\sin[x(4n-1)^{1/2}][1+\mathcal{O}(|2n-\tfrac{1}{2}|^{-1/2})]\,. \tag{3.59}$$

Note that

$$|S_n|\le S_n^0\,, \tag{3.60}$$

where

$$S_n^0\equiv\frac{(\beta^2/R_0{}^2)^n}{n}\left[\frac{x}{\pi}\right]^{1/2}e^{-x^2/2}[1+a/(2n-\tfrac{1}{2})] \tag{3.61}$$

for some finite value a.

By comparing the geometric series F_g

$$F_g=\sum_{n=0}^{\infty}r^n<\infty\,,\quad\text{for}\ |r|<1\,, \tag{3.62}$$

with the series F_M^0 defined by

$$F_M^0\equiv\sum_{m=M}^{\infty}S_n^0\,. \tag{3.63}$$

It is clear that for some $M<\infty$, F_M^0 converges absolutely for all x provided

$$|\beta/R_0|<1\,. \tag{3.64}$$

Since the terms S_n^0 dominate S_n, the function $\zeta^+(z)$ converges absolutely for $|\beta/R_0|<1$. Physically this restriction is roughly equivalent to a statement about the relative ranges of the nucleon-nucleon interaction and the size of the nuclear bound system.

At intermediate energies Vary and Dover[45] have found for the parametrization [Eq. (3.36)] of the scattering amplitude $A(\vec{q})$ that the range β of the nucleon-nucleon interaction is 1.2—1.6 fm. Nuclear radii from helium through lead range from 1.9—5.5 fm. Thus the function $\zeta^+(z)$ is well behaved even for small nuclear systems.

In Fig. 3 the behavior of $\zeta^+(z)$ as a function of R_0 is displayed. Note the smooth transition from the average value of $\zeta^+(0)=0.5$ to the maximum of 1.0. At $z=R_0$ the function $\zeta^+(z)$ appears to attain approximately 90% of the asymptotic value $\zeta^+(\infty)$

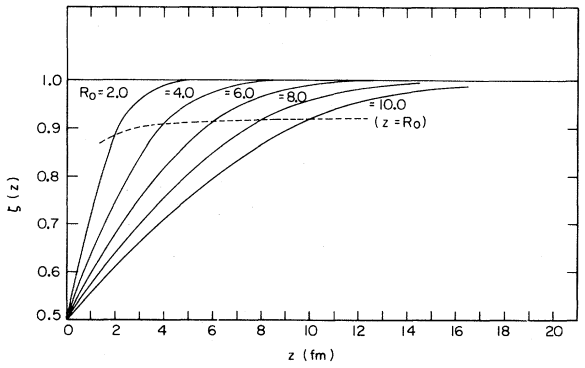

FIG. 3. Behavior of the transparency $\zeta(z)$ for fixed $\beta=1.4$ fm as the nuclear size parameter R_0 varies.

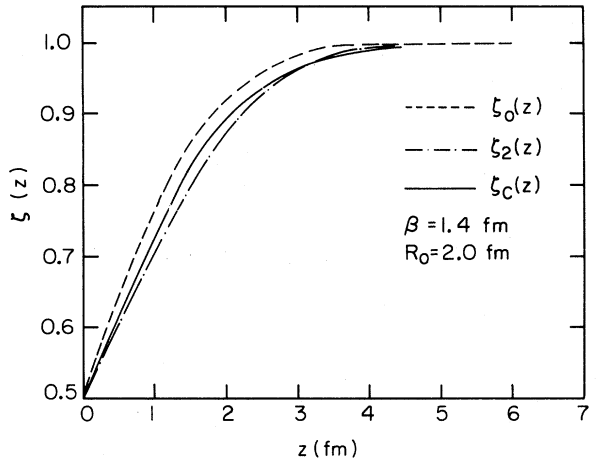

FIG. 4. Convergence of the transparency function $\zeta(z)$. The dashed curve gives the zeroth order results, the dotted-dashed curve displays the second order effects, and the solid curve shows the converged result. Parameters are $\beta=1.4$ fm and $R_0=2.0$ fm.

for $R_0>2.$ fm.

A question of considerable importance for realistic densities is the rate of convergence of the series for $\zeta^+(z)$ as a function of the nuclear size. In Fig. 4 we compare the results of using $w_0^+(z)$, $(w_0^+(z)+w_2^+(z))$, and $w^+(z)$ to obtain the function $\zeta^+(z)$. Notice in Fig. 4 that for the worst possible rate of convergence of $\zeta(z)$ (i.e., R_0 small), the difference between the zeroth order result and the second order result is quite small. A better way of viewing the difference is to consider the ratio of zeroth and second order terms to the converged result. From Fig. 5 we can see that the maximum discrepancy in the zeroth order case is $\sim 5\%$, whereas for the second order case it is $\sim 3\%$ for $R_0=2$ fm. Furthermore, as R_0 increases to 4 fm the maximum discrepancy is of the order of $\sim 1.6\%$ and even smaller for $R_0=6$ fm. We conclude that within the accuracy of the parametrization, the function $\zeta^+(z)$ is adequately described by retaining only the first term. This is equivalent to approximating the distortion functions $w^{\pm}(\vec{r})$ by the first term alone, i.e.,

$$w^{\pm}(\vec{r})\simeq\gamma(b)\theta^{\pm}(z) . \tag{3.65}$$

Except for the very smallest nuclear systems, the approximation of Eq. (3.65) should be satisfactory. This conclusion is reinforced by noting that real nuclear densities may be expected to be considerably softer than are Gaussian densities. The equivalent R_0 values are larger and the convergence enhanced.

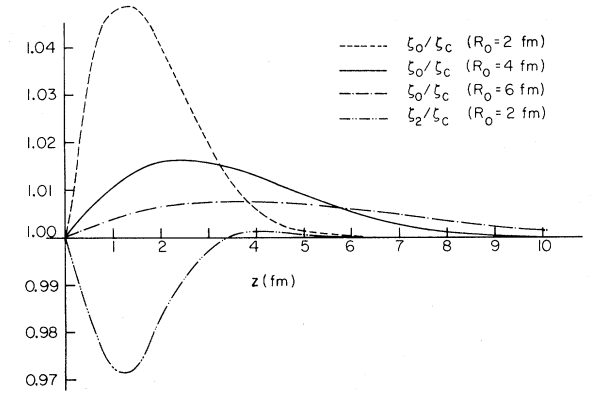

FIG. 5. Comparison of the ratio of the unconverged transparency to the converged result as a function of nuclear size R_0. The dashed curve gives the ratio ζ_0/ζ_c for $R_0=2$ fm. Similarly the solid curve is for ζ_0/ζ_c at $R_0=4$ fm and the dotted-dashed curve is for ζ_0/ζ_c at $R_0=6$ fm. Finally, the dashed-dotted-dotted curve is for ζ_2/ζ_c at $R_0=2$ fm. The parameter $\beta=1.4$ fm.

D. Study of the zero range truncation

In the preceding subsection we discussed the convergence of the nucleon distortion functions when folded with the nuclear density. This subsection compares the total finite range calculation and the zero range trunction. General features and behavior of the differential cross section are discussed within a simplified model calculation.

We begin by noting the approximations made for the distortion operator W. Using Eqs. (2.46), (3.15), (3.16), and (3.19) the operator W becomes

$$W=\prod_{j\in B}(1+\bar{w}_j) , \tag{3.66}$$

where

$$\bar{w}_j=(1-w_{pj}^-)(1-w_{nj}^-)(1-w_{pj}^+)-1 . \tag{3.67}$$

Upon using the approximation Eq. (3.65) and the properties of $\theta^{\pm}$ functions the nucleon factor $\bar{w}_j$ becomes

$$\begin{aligned}\bar{w}_j(\vec{r}_j,\vec{r}_p,\vec{r}_n)=&-\gamma_{pj}(\vec{b}_j-\vec{b}_p)\\&-\theta^-(z_n-z_j)\gamma_{nj}(\vec{b}_n-\vec{b}_j)\\&+\theta^-(z_n-z_j)\gamma_{nj}(\vec{b}_n-\vec{b}_j)\gamma_{pj}(\vec{b}_p-\vec{b}_j) .\end{aligned} \tag{3.68}$$

We further simplify Eq. (3.68) by replacing θ^- by its average value $\frac{1}{2}$; thus

$$\begin{aligned}\bar{w}_j\approx&-\gamma_{pj}(\vec{b}_{pj})-\tfrac{1}{2}\gamma_{nj}(\vec{b}_{nj})\\&+\tfrac{1}{2}\gamma_{nj}(\vec{b}_{nj})\gamma_{pj}(\vec{b}_{pj}) .\end{aligned} \tag{3.69}$$

The function $\gamma(b)$ is of the form given by Eq. (3.38);

TABLE III. The nucleon-nucleon cross sections σ^{tot} and α values used for energy dependent comparison of finite range vertex functions and the zero-range truncation. The values listed in this table correspond to the values used in tests of finite range vertex function versus zero-range truncation computed through first order in density. They represent average values of these quantities at these energies. Some variation from accepted values may be expected.

Incident kinetic energy (MeV)	$\sigma^{\text{tot}}(+)$ (fm^2)	$\sigma^{\text{tot}}(-)$ (fm^2)	$\alpha(+)$	$\alpha(-)$
50	5.00	5.00	1.87	1.87
100	5.00	5.00	1.87	1.87
300	3.50	4.00	0.60	1.00
500	3.46	4.30	0.55	0.800
700	4.23	3.00	0.20	0.600
800	4.32	3.50	0.144	0.600
1050	4.39	3.46	−0.073	0.550

the values for σ^{tot}, α, and β are taken as the appropriate average values for protons and neutrons of specified kinetic energy. From the study of Vary and Dover[45] the range parameter β was found to be comparatively insensitive for wide variations in energy. In the model calculation, $\beta=1.24$ fm is used. Values for σ^{tot} and α are listed in Table III.

The total distortion function W can be written as a series in the number of target nucleons participating in the scattering:

$$W=1-\sum_{j\in B}\bar{w}_j+\sum_{j\neq k}\bar{w}_j\bar{w}_k-\sum_{j\neq k\neq l}\bar{w}_j\bar{w}_k\bar{w}_l+\cdots . \tag{3.70}$$

Recall that the function W appears in the integrated distortion factor

$$F^{L_B m_B}_{\lambda_B \nu_B}(\vec{r}_p,\vec{r}_n) ,$$

Eq. (2.39). Consider only diagonal scattering, i.e.,

$$(L_B m_B)=(\lambda_B \nu_B) .$$

$$F(\vec{r}_p,\vec{r}_n)=\int \rho^{(B)}(\vec{r}_1,\vec{r}_2\cdots\vec{r}_B)\times W(\vec{r}_p,\vec{r}_n,\vec{r}_1\cdots\vec{r}_B)\times d^3r_1\cdots d^3r_B . \tag{3.71}$$

Substitution of Eq. (3.70) into Eq. (3.71) yields a spectator expansion in the residual target density.

$$F(\vec{r}_p,\vec{r}_n)=1+f_1(\vec{r}_p,\vec{r}_n)+f_2(\vec{r}_p,\vec{r}_n)+\cdots f_B(\vec{r}_p,\vec{r}_n) \tag{3.72}$$

and

$$f_n(\vec{r}_p,\vec{r}_n)=(-)^n\int \rho^{(n)}\bar{w}_1\bar{w}_2\cdots\bar{w}_n\times d^3r_1\cdots d^3r_n , \tag{3.73}$$

where $\rho^{(n)}$ is the n-body density of the residual target. This density expansion introduces ground state nucleon correlations. The scattering of the entrance proton or the final deuteron from one target nucleon to another may be modulated by strong short range correlations existing between the spectators of the residual target.

Further simplifications are possible for the distortion factor F. We list the ones used for demonstrating the properties and behavior of the cross section

$$F_0=1 \text{ (plane wave)} , \tag{3.74}$$

$$F_1=1+f_1 \text{ (1st order)} , \tag{3.75}$$

$$F_2=1+f_1+f_2 \text{ (2nd order, no correlations)} . \tag{3.76}$$

If the many body density is factorable, i.e.,

$$\rho^{(n)}=\prod_{i=1}^{n}\rho^{(1)}(i) , \tag{3.77}$$

then

$$F_T=(1+f_1)^B . \tag{3.78}$$

We parametrize the correlated two body density in the form

TABLE IV. Gaussian fit coefficients of a $1p_{3/2}$ neutron wave function generated from a density dependent Hartree-Fock calculation for ^{12}C.

Form: $U(r)=r^2\sum_{j=1}^{M}C_j^n\exp(-\alpha_j^n r^2)$.

$M=13$. $E+n$ denotes 10^{+n}.

j	C_j^n	α_i^n
1	0.253409468E+00	0.2100E+01
2	−0.192559749E+01	0.1040E+01
3	−0.362778021E−01	0.4300E+01
4	−0.256284978E+02	0.5400E+00
5	−0.356354807E+01	0.3450E+00
6	0.749165310E+00	0.2340E+00
7	0.170216948E+02	0.4550E+00
8	0.134197792E+02	0.6560E+00
9	0.113537630E+00	0.7820E−01
10	−0.194835052E+00	0.6607E−01
11	0.194423435E+00	0.5700E−01
12	−0.128898899E+00	0.5000E−01
13	0.475755771E−01	0.4650E−01

TABLE V. Gaussian fit coefficients for realistic Hartree-Fock ^{11}C density, normalized to unity.

Form: $\rho(r)=\sum_{j=1}^{M} C_j(\alpha_j/\pi)^{3/2}\exp(-\alpha_j r^2)$,

$$\sum_{j=1}^{M} C_j=1 .$$

$M=10$. $E+n$ denotes 10^{+n}.

j	C_j	α_j
1	0.411334549E −03	0.741894153E −01
2	0.845453470E −01	0.148378831E +00
3	−0.546794586E +00	0.222568246E +00
4	0.663778679E +01	0.296757661E +00
5	−0.264960114E +02	0.370947076E +00
6	0.604007273E +02	0.445136492E +00
7	−0.641846813E +02	0.519325907E +00
8	0.241154588E +02	0.593515322E +00
9	0.583670412E +01	0.667704738E +00
10	−0.484814650E +01	0.741894153E +00

$$\rho_c^{(2)}=\rho^{(1)}(1)\rho^{(1)}(2)N[1-\lambda_c\exp(-\beta_c r_{12}^2)] . \tag{3.79}$$

N is a normalization, λ_c is the correlation strength,

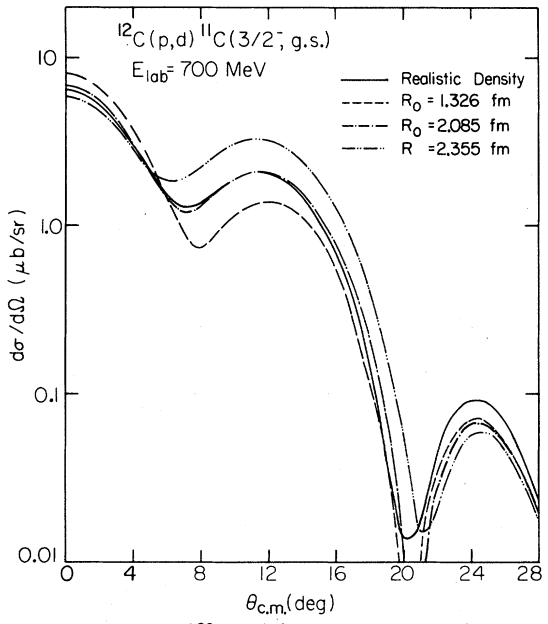

FIG. 6. Differential cross section of ^{12}C$(p,d)^{11}$C$(\frac{3}{2}^-$,g.s.) at 700 MeV for different densities in the distortion functions. The solid curve is the result for the realistic density from DDHF. The remaining three curves are the results obtained using a single parameter (R_0) Gaussian density, where $R_0=1.326$, 2.085, and 2.355 fm.

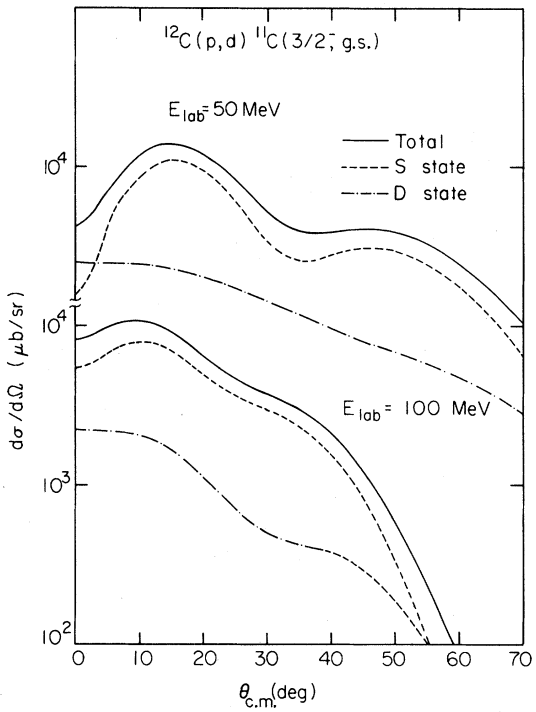

FIG. 7. Differential cross section of ^{12}C$(p,d)^{11}$C$(\frac{3}{2}^-$,g.s.) at 50 and 100 MeV proton kinetic energy. The solid curve is the total differential cross section, whereas the dashed and dotted-dashed curves display the pure S-state and D-state contributions, respectively.

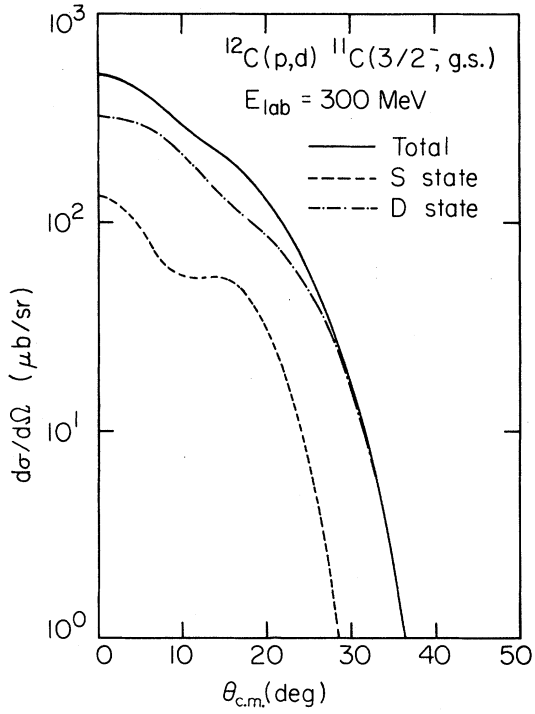

FIG. 8. Same as Fig. 7, except $E_{lab}=300$ MeV.

and β_c is a measure of the correlation range. Thus

$$F_{2c}=1+f_1+f_{2c}\ . \tag{3.80}$$

To evaluate the finite range transition amplitude we employ F_1, and express the target density as a sum of Gaussians, in which case F_1 becomes an expression in Gaussians. Then the transition amplitude becomes an analytic function expressed in terms of the double folded asymmetric Gaussian transform discussed in Appendix C.

Consider the sensitivity of the cross section in this model to the details of the density. Table IV contains the coefficients for the residual target density of ^{11}C fit to a sum of Gaussians. The density for ^{12}C was generated by a density dependent Hartree-Fock code,[46] and the density of the residual target was obtained by subtraction of the single particle density of the captured neutron. The values used for the total nucleon-nucleon cross section ($\sigma^{\rm tot}$) and alpha (α) are given in Table III. Figure 6 displays the results of using the realistic density (Table V) as opposed to single Gaussian densities with $R_0=1.826$, 2.085, and 2.355 fm. Notice that for $R_0=2.085$ fm the cross section is virtually identical to that of the realistic density. This suggests employing a single Gaussian density adjusted to yield results close to those of the realistic density in lowest order, in order to simplify the higher order terms of Eq. (3.72).

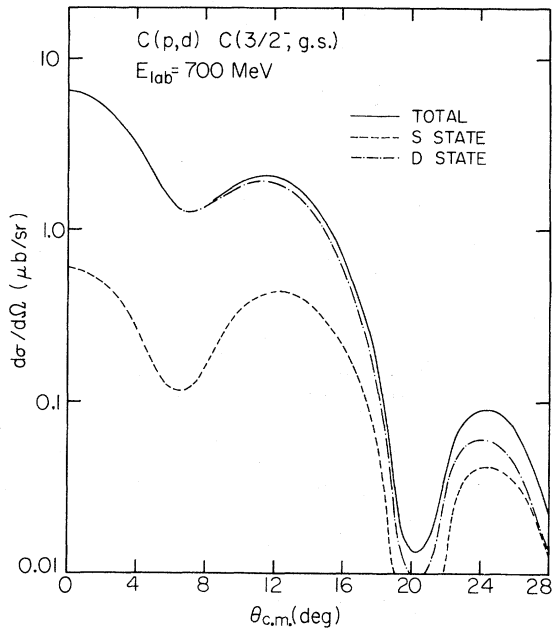

FIG. 10. Same as Fig. 7, except $E_{\rm lab}=700$ MeV.

In Figs. 7—11 we observe the relative importance of *S*- and *D*-state contributions to the differential cross section in the reaction ^{12}C$(p,d)^{11}$C$(\frac{3}{2}^-$,g.s.) for proton laboratory energies ranging from 50 MeV to 1.05 GeV.

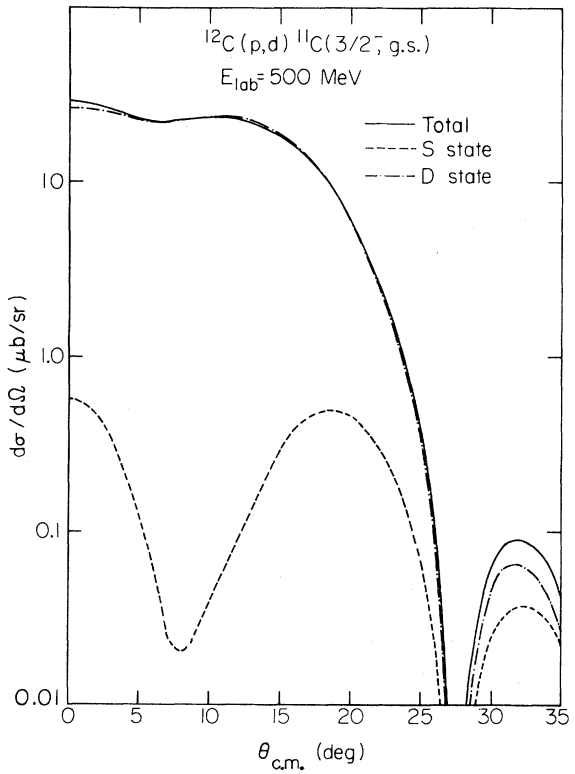

FIG. 9. Same as Fig. 7, except $E_{\rm lab}=500$ MeV.

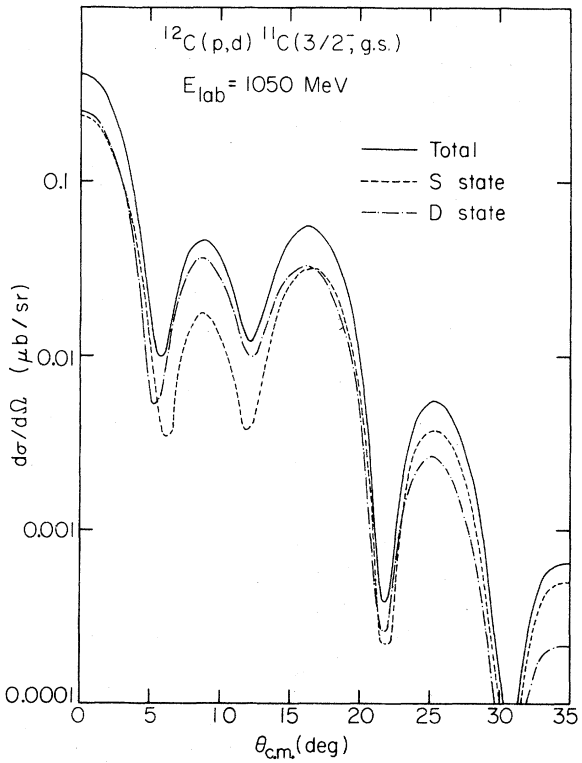

FIG. 11. Same as Fig. 7, except $E_{\rm lab}=1050$ MeV.

At 100 MeV the D state already provides about 15% of the cross section. Between 300 and 700 MeV the cross section is dominated by the D state with very little S-state contribution. Note that in this simplified model calculation the shapes of the S and D state cross sections resemble each other. Had we included spin-orbit pieces to the distortion, there might have been stronger disparities between these two contributions.

How sensitive are the results to the zero-range truncation? In Figs. 12—17 the reaction cross sections calculated using F_1, and the realistic density (Table IV) are displayed for both FR and ZRT. It is notable that throughout the energy range 50 MeV—1.05 GeV, the ZRT resembles very closely the results of the FR calculation. For order of magnitude effects and qualitative features, the ZRT reproduces the FR calculations throughout the energy range examined. We conjecture that the first order correction to ZRT given by Eq. (3.14) should be adequate to reproduce the FR calculation throughout

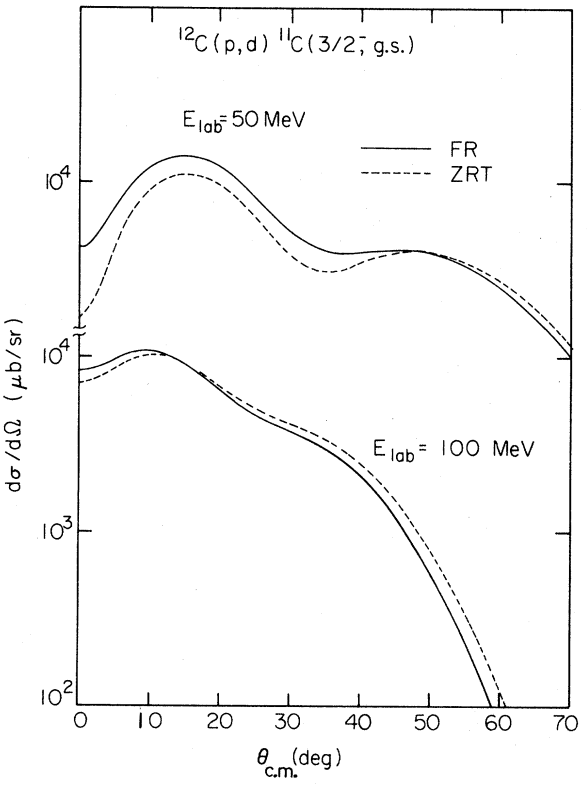

FIG. 12. Differential cross section for $^{12}C(p,d)^{11}C(\frac{3}{2}^-,\text{g.s.})$, $E_{lab}=50$ and 100 MeV. The solid curve displays the results for the finite range (FR) calculation, whereas the dashed curve shows the results using the zero-range truncation (ZRT).

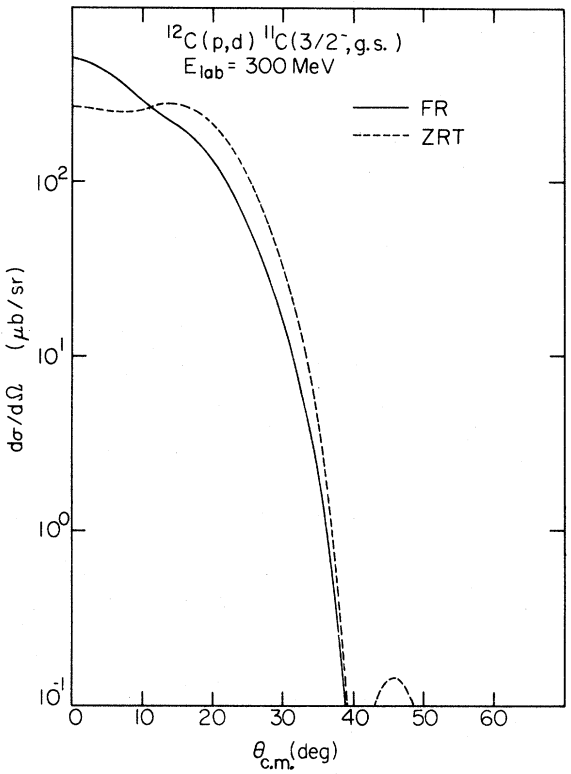

FIG. 13. Same as Fig. 12, except $E_{lab}=300$ MeV.

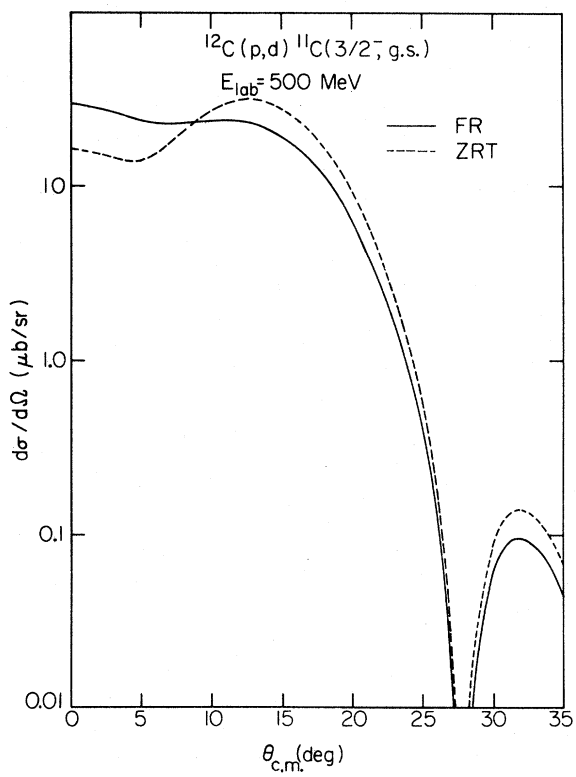

FIG. 14. Same as Fig. 12, except $E_{lab}=500$ MeV.

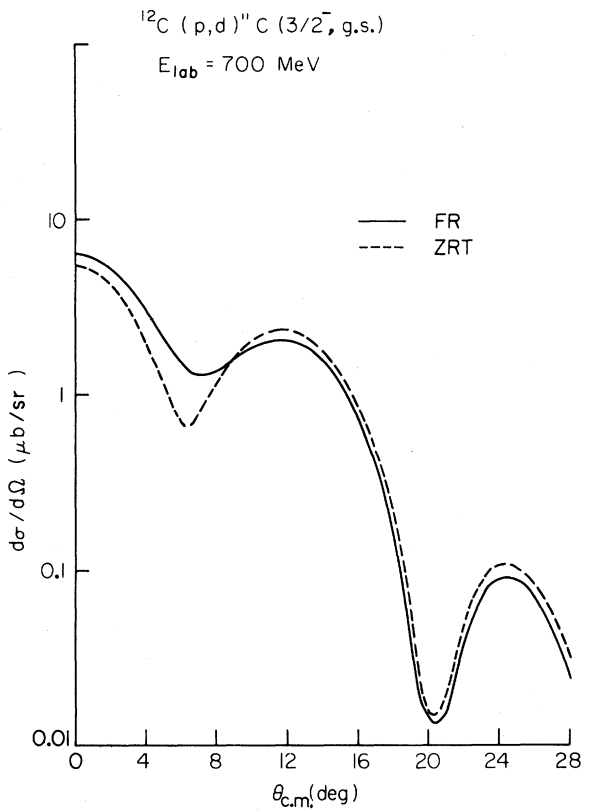

FIG. 15. Same as Fig. 12, except $E_{lab}=700$ MeV.

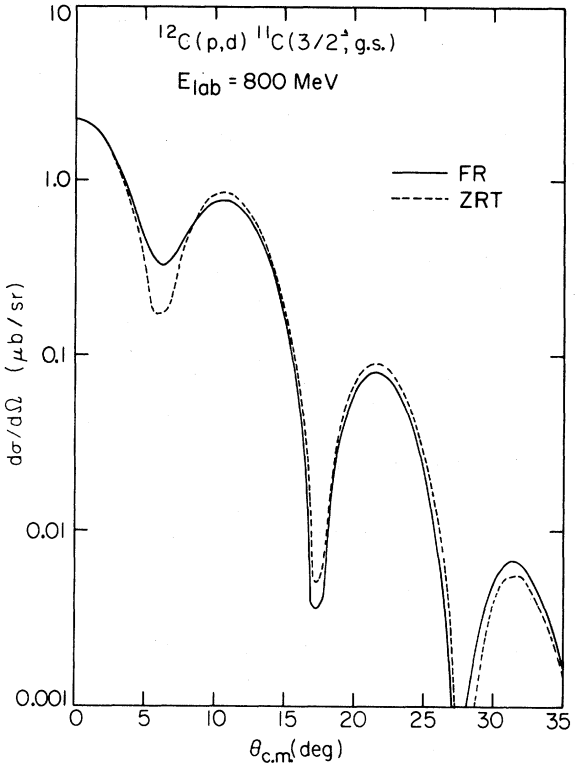

FIG. 16. Same as Fig. 12, except $E_{lab}=800$ MeV.

the energy range.

Thus far we have examined general features of the cross section pertaining to the energy dependence and its sensitivity to the deuteron S and D state mixture using a simple first order calculation retaining only the lowest order distortion effects in the density expansion. We now address the sensitivity to the density expansion of the distortion function F using the ZRT for simplicity. In Fig. 18 we compare the cross section obtained using a plane wave (F_0), a first order (F_1), a second order (F_2), and iterated first order calculation in the distortion. As can be seen, all calculations produce the diffractive features associated with optical-like scattering from a black disk. We see that the iterated first order distortion and the second order distortion are virtually identical through the second maxima. Thus convergence of the density expansion appears to be quite rapid. Third order contributions may be expected to be significant in the third maxima and beyond.

Figure 19 compares a ZRT calculation using F_2 and F_{2c}, where $\lambda_c=1$ and $\beta_c=0.60$ fm^{-2} in Eq. (3.79). As can be seen, the difference is small. This leads us to conclude that it will be difficult to extract meaningful information about short range correlations from these reactions unless all in-

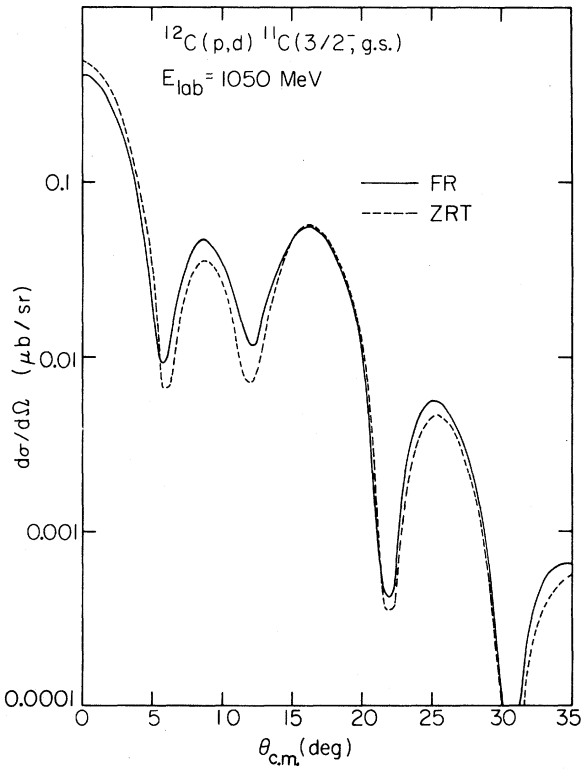

FIG. 17. Same as Fig. 12, except $E_{lab}=1050$ MeV.

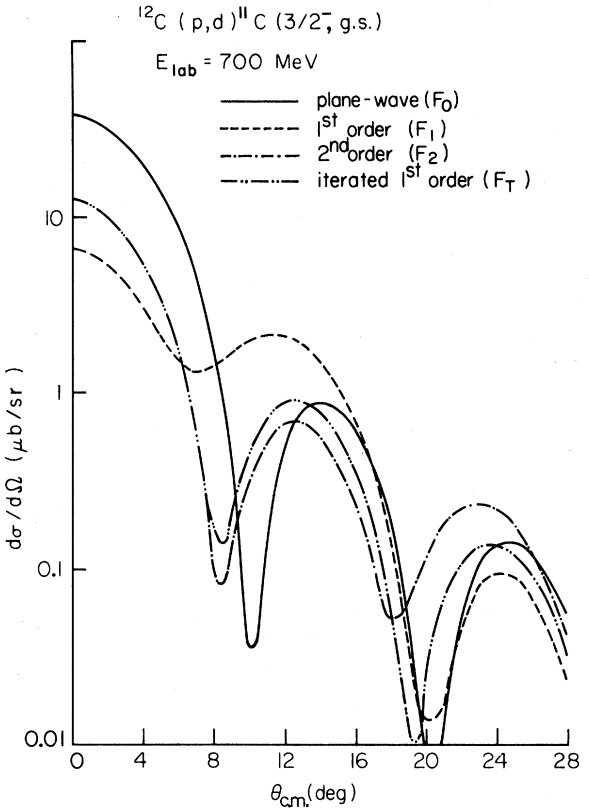

FIG. 18. Differential cross section for $^{12}C(p,d)^{11}C(\frac{3}{2}^-,g.s.)$, $E_{lab}=700$ MeV. The solid curve corresponds to the plane wave calculation; that is, $F=F_0=1$, which is no distortion of the proton or deuteron waves. The dashed curve displays results of including only first order distortion effects. The dashed-dotted curve shows the effect including short range correlations in a second order calculation of the density. Finally, the dashed-dotted-dotted curve shows the iterated first order result (with no correlations).

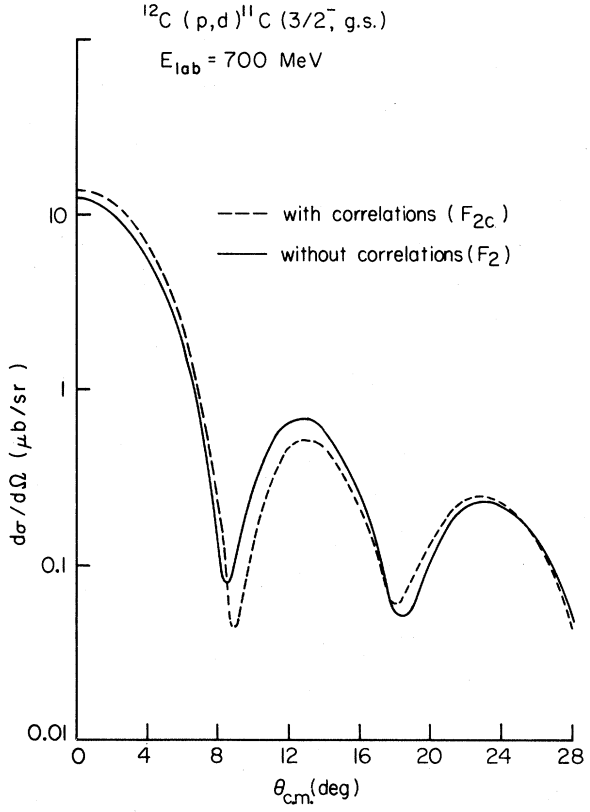

FIG. 19. Comparison of effect on cross section when short range correlations are included (dashed curve) and not included (solid curve) in a second order calculation.

gredients in the reaction are developed accurately. This conclusion is consistent with recent DWBA studies[47] of $^{16}O(d,p)^{17}O$ at 700 MeV which demonstrated large sensitivity to uncertainties in the neutron wave function and to uncertainties in the deuteron optical potential.

Finally, we tested the sensitivity to the density in a second order (F_2) ZRT calculation. For a single Gaussian density with $R_0=2.085$ fm (cf. Fig. 6) we again find a close resemblance with results using the realistic density.

IV. CONCLUSIONS

We have presented a multiple scattering framework for transfer reactions in which certain important physical mechanisms may be addressed specifically and developed for the (p,d) process. We have developed a format for handling the deuteron vertex function in a fashion which permits evaluation of both the S and D state contributions to the reaction amplitude on a microscopic basis. Using simple model assumptions we have examined the energy dependence of the reaction cross section to S and D state contributions. For intermediate energies (50 MeV–1. GeV) we have seen that neglecting the D-state contribution to the (p,d) reaction amplitude is not suitable. At about 500 MeV the cross section arises almost purely from the D state. Thus for a realistic treatment of the (p,d) cross section it is necessary to include the D-state contribution.

For qualitative features and order of magnitude effects we have demonstrated that the ZRT appears to present a feasible alternative to the FR calculation. Furthermore, we feel that the first order correction to the ZRT discussed in Sec. III A may alleviate the need for FR calculations, and we are investigating this correction with more realistic distortions in which we plan to include the spin orbit dependence of the nucleon-nucleon amplitude. In this context we plan to study the (p,d) reaction from

two approaches. The first approach is to use conventional parametrizations of optical potentials which reproduce elastic and inelastic scattering and asymmetries as a guide to the input into this (p,d) formulation. The alternative approach is more microscopic, and involves generating the nucleon-nucleon distortion functions from realistic nucleon-nucleon t-matrix amplitudes, which reproduce the low and intermediate energy nucleon-nucleon phase shifts. The first approach is most suitable at higher energies where optical potentials may be readily expressed in terms of nuclear densities and have been successfully used to predict elastic and inelastic cross sections in the eikonal framework. Within our framework, higher order correlation effects are found to be negligible and this affords a more convenient microscopic approach to nuclear transfer cross sections and polarizations.

APPENDIX A: OPERATOR IDENTITIES

Let H_0 be the Hamiltonian governing a set of noninteracting particles; then $H_j=H_0+V_j$, where V_j denotes the specific interparticle interactions incorporated in H_j. There exists an associated Green's function defined by

$$G_j(z)=(z-H_j)^{-1}\,, \tag{A1}$$

where z is the usual complex energy parameter which specifies the incoming or outgoing boundary conditions as $z\rightarrow E_j\pm i\epsilon$. We define V_{jk} as the difference between two Hamiltonians:

$$V_{jk}=H_j-H_k\,. \tag{A2}$$

The operator identity defined by

$$a=b+b(b^{-1}-a^{-1})a \tag{A3}$$

implies that the Green's functions G_j and G_k are related by

$$G_j=G_k+G_k(H_j-H_k)G_j=G_k+G_kV_{jk}G_j\,. \tag{A4}$$

Furthermore, the operator inverses are related by

$$G_j^{-1}=G_k^{-1}+H_k-H_j=G_k^{-1}+V_{jk}\,. \tag{A5}$$

Consider $\{h_j\}$ to be the subset of $\{H_j\}$, defining a channel in which the particles are partitioned into two noninteracting self-bound clusters. For each h_j there exists a set of two-cluster interactions denoted $\{v_j^l\}$, where the index (l) denotes the different cluster-cluster interactions. For example, the cluster-cluster interactions could represent optical potentials or more fundamental particle-particle processes possible in many body systems. From these interactions we construct a set of interaction Hamiltonians, defined by

$$h_j^l=h_j+v_j^l\,. \tag{A6}$$

The Green's functions associated with h_j and h_j^l are denoted by g_j and g_j^l, respectively.

The ket vectors $|\phi_j(\alpha)\rangle$ are defined to be the eigensolutions of channel (j) and state (α) of the eigenequation

$$[E_j(\alpha)-h_j]\,|\phi_j(\alpha)\rangle=0\,. \tag{A7}$$

The ket vectors $|\chi_j^{l(\pm)}(\alpha)\rangle$, are solutions to the eigenequation

$$[E_j(\alpha)-h_j^l]\,|\chi_j^{l(\pm)}(\alpha)\rangle=0\,. \tag{A8}$$

In the following development the $(\pm)$ indexing on the scattered states (and the Green's functions) shall be suppressed for simplicity, unless necessary for precision. The ket vectors $|\chi_j^l(d)\rangle$ are obtained in the conventional way from

$$|\chi_j^l(\alpha)\rangle=|\phi_j(\alpha)\rangle+g_j^lv_j^l\,|\phi_j(\alpha)\rangle\,. \tag{A9}$$

This may be written as

$$|\chi_j^l(\alpha)\rangle=g_j^l\{[g_j^l]^{-1}+v_j^l\}\,|\phi_j(\alpha)\rangle\,.$$

Then, using Eq. (A5)

$$|\chi_j^l(\alpha)\rangle=g_j^lg_j^{-1}\,|\phi_j(\alpha)\rangle\,. \tag{A10}$$

The inverse equation is

$$|\phi_j(\alpha)\rangle=g_j[g_j^l]^{-1}\,|\chi_j^l(\alpha)\rangle\,. \tag{A11}$$

Using Eq. (2.11) for ϕ and l' leads to

$$|\chi_j^l(\alpha)\rangle=g_j^l[g_j^{l'}]^{-1}\chi_j^{l'}(\alpha)\rangle\,. \tag{A12}$$

Equation (A12) describes the connection between two scattered waves evolving from the same two-cluster channel under the influence of different cluster interactions. Suppose that v_j^l is the "exact" microscopic interaction between two nuclei, and that $v_j^{l'}$ is some optical model potential. Then Eq. (A12) describes the connection between the exact scattering vector and the model vector. It provides a starting point for a study of the differences between the many-body wave vector and any model wave vector. The many body operator $g_j^l[g_j^{l'}]^{-1}$ may be treated by the spectator expansion or other decomposition methods. Thus, the framework outlined above is suitable for studying the many body aspects of the problem in a systematic manner.

APPENDIX B: DEUTERON VERTEX FUNCTIONS

A modern realistic nucleon-nucleon interaction V_{NN} contains at least spin, isospin, spin-orbit, and

tensor coupling terms. Such couplings even in the presence of a soft core render the utilization of these interactions in the formation of transition amplitudes extremely cumbersome. For general usage in reactions, it is desirable to obtain from V_{NN} and its corresponding deuteron wave function ϕ_{dtn} a quantity which is approximately "invariant"; that is, which essentially contains all the deuteron properties, but may be regarded as comparatively insensitive to the detailed features of the interaction. These functions we call the deuteron vertex function.

For the $({}^3S_1\text{-}{}^3D_1)$ configuration, a typical realistic potential such as the Reid[48] potential can be abbreviated

$$V_{NN}=V_C+V_T S_{12}+V_{LS}L\cdot S\ , \tag{B1}$$

and the deuteron wave function is written as

$$\phi_{dtn}(1,M_J)=\frac{1}{r}[X_{1M_J}Y_{00}U_S(r)+\sum_{m_D\mu_S}\langle 1M_J\,|\,2m_D1\mu_S\rangle X_{1\mu_S}Y_{2m_D}(r)W_D(r)]\ . \tag{B2}$$

The deuteron vertex functions d_{lm_l} are defined as the angular momentum decoupled product of $D_{Jm_j}=V_{NN}\phi_{dtn}$. That is,

$$D_{1m_J}(\vec{r},\tilde{\sigma})=X_{1m_J}Y_{00}\left[\frac{1}{r}U_S^{\rm eff}(r)\right]+\sum_{m_D,\mu_S}\langle 1m_J\,|\,2m_D1\mu_S\rangle\times X_{1\mu_S}Y_{2m_D}(r)\left[\frac{1}{r}U_D^{\rm eff}(r)\right]\ , \tag{B3}$$

where

$$U_S^{\rm eff}(r)=V_C(r)U_S(r)+\sqrt{8}V_T(r)W_D(r) \tag{B4}$$

and

$$U_D^{\rm eff}=(V_C(r)-2V_T(r)-3V_{LS}(r))W_D(r)+\sqrt{8}V_T(r)U_S(r)\ . \tag{B5}$$

An alternative expression for Eq. (B3) in terms of the vertex functions is

$$D_{1m_S}=X_{1m_J}d_{00}(\vec{r})+\sum\langle 1m_J\,|\,2m_D1\mu_S\rangle X_{1\mu_S}d_{2m_D}(\vec{r})\ , \tag{B6}$$

where

$$d_{00}(\vec{r})=Y_{00}\frac{1}{r}U_S^{\rm eff}(r) \tag{B7}$$

and

$$d_{2m_D}(\vec{r})=Y_{2m_D}(\hat{r})\frac{1}{r}U_D^{\rm eff}(r)\ . \tag{B8}$$

The vertex functions $d_{lm_l}(\vec{r})$ are simpler to work with than is the deuteron potential V_{NN}.

While the interaction V_{NN} is known analytically, the corresponding wave functions are generated on a numerical mesh. Thus the functions $U_L^{\rm eff}(r)$ are known numerically, rather than analytically. A convenient parametrization for these functions is given in Tables I and II.

APPENDIX C: ANALYTIC EXPRESSION FOR THE FOURIER TRANSFORM OF FOLDED SPHERICAL HARMONICS IN AN ASYMMETRIC GAUSSIAN FIELD

The harmonic folded integral in a deformed Gaussian field is defined as

$$I(Q{:}LM;P{:}lm)\equiv\int e^{i\vec{Q}\cdot\vec{R}}(R)^L Y_{LM}^*(\hat{R})e^{i\vec{P}\cdot\vec{r}}(r)^l\times Y_{lm}(r)E(\vec{R},\vec{r})d^3R\,d^3r\ , \tag{C1}$$

where

$$E(R,r)\equiv\exp\{-A_xX^2-A_yY^2-A_zZ^2+2B_xxX+2B_yyY+2B_zzZ-a_xx^2-a_yy^2-a_zz^2\}. \tag{C2}$$

In Eq. (C1) the $Y_{LM}(\hat{R})$ are the standard spherical harmonics, obeying the normalization convention

$$\int Y_{LM}^*(\hat{R})Y_{L'M'}(\hat{R})d\Omega_R=\delta_{LL'}\delta_{MM'}\ , \tag{C3}$$

and satisfying the identity

$$Y_{LM}^*(\hat{R})=(-)^M Y_{L(-M)}(\hat{R})\ . \tag{C4}$$

For arbitrary angular momentum states (LM) and (lm), the integral of Eq. (C1) is cumbersome. Consequently it is desirable to replace it by a representation in which the angular momentum dependence does not appear explicitly in the integral, but is subsumed in a set of differential operators.

A general polynomial differential operator of rank l and order m, denoted by $D_{lm}(\vec{q})$, may be defined in the following form:

$$D_{lm}(\vec{q}) \equiv \sum_{\alpha+\beta+\gamma=l} a^{lm}_{\alpha\beta\gamma}(\partial/\partial q_x)^{\alpha} \times(\partial/\partial q_y)^{\beta}(\partial/\partial q_z)^{\gamma} . \quad \text{(C5)}$$

By requiring the D_{lm} to satisfy the following expressions,

$$D_{lm}(\vec{q})e^{i\vec{q}\cdot\vec{r}} = (r)^l Y_{lm}(\hat{r})e^{i\vec{q}\cdot\vec{r}} \quad \text{(C6a)}$$

and

$$D^*_{lm}(\vec{q})e^{i\vec{q}\cdot\vec{r}} = (r)^l Y^*_{lm}(\hat{r})e^{i\vec{q}\cdot\vec{r}} , \quad \text{(C6b)}$$

then for a given (lm), the coefficients $a^{lm}_{\alpha\beta\gamma}$ are completely determined. Furthermore, using Eqs. (C4) and (C6b), the following identity is obtained:

$$D_{lm}(\vec{q})^* = (-)^m D_{l-m}(\vec{q}) . \quad \text{(C7)}$$

Using Eqs. (C6a) and (C6b), Eq. (C1) may be rewritten as

$$I(\vec{Q}:LM;\vec{P}:lm) = D^*_{LM}(\vec{Q})D_{lm}(\vec{P})\mathcal{I}(\vec{Q},\vec{P}) , \quad \text{(C8)}$$

where

$$\mathcal{I}(\vec{Q},\vec{P}) \equiv \int e^{i\vec{Q}\cdot\vec{R}}e^{i\vec{P}\cdot\vec{r}}E(\vec{R},\vec{r})d^3R\, d^3r . \quad \text{(C9)}$$

Note that in Eq. (C8) the angular momentum dependence has been removed from the integral of Eq. (C1). The integral $\mathcal{I}(\vec{Q},\vec{P})$ is the double Fourier transform of the coupled asymmetric Gaussian form factor $E(\vec{R},\vec{r})$. Evaluating Eq. (C9) yields

$$\mathcal{I}(\vec{Q},\vec{P}) = \pi^3 I_x(Q_x,P_x)I_y(Q_y,P_y)I_z(Q_z,P_z) , \quad \text{(C10)}$$

where

$$I_j(Q_j,P_j) = \left[\frac{1}{A_jA_j - B_j^2}\right]^{1/2} \exp\left[-\frac{1}{4(A_jA_j-B_j^2)}(Q_j^2A_j + P_j^2A_j + 2P_jQ_jB_j)\right] \quad \text{(C11)}$$

and j may be x, y, or z.

Thus the harmonic folded integral $I(\vec{Q}:LM;\vec{P}:lm)$ has been reduced to a general analytic expression in which the differential operators D_{lm} and D_{LM} project the desired angular momentum coupling.

APPENDIX D: GAUSSIAN FITS TO FUNCTIONS

In order to ensure speed and accuracy in numerical calculations we have least squares fits of analytical functions with carefully selected asymptotic forms to a number of intermediate numerical functions employed in our analyses. For convenience to other investigators we present the results of these fits in Tables I, II, IV, and V.

[1]G. J. Igo, Rev. Mod. Phys. 50, 523 (1978).
[2]D. Z. Freedman, C. Lovelace, and J. M. Namyslowski, Nuovo Cimento 43A, 258 (1966).
[3]P. Grassberger and W. Sandhas, Nucl. Phys. B2, 181 (1967).
[4]E. O. Alt, P. Grassberger, and W. Sandhas, Nucl. Phys. B2, 167 (1967).
[5]E. F. Redish, Nucl. Phys. A235, 82 (1974).
[6]D. J. Kouri and F. S. Levin, Phys. Rev. C 16, 556 (1977).
[7]Gy. Bencze and P. C. Tandy, Phys. Rev. C 16, 564 (1977).
[8]K. L. Kowalski, Phys. Rev. C 16, 1735 (1977).
[9]K. M. Watson, Phys. Rev. 89, 575 (1953).
[10]R. J. Glauber, in *Lectures in Theoretical Physics,* edited by W. E. Brittin and L. G. Dunham (Interscience, New York, 1959), Vol. I.
[11]A. K. Kerman, H. McManus, and R. M. Thaler, Ann. Phys. (N.Y.) 8, 551 (1959).
[12]O. Kofoed-Hansen, Nuovo Cimento 60A, 621 (1968).
[13]J. Formanek, Nucl. Phys. B12, 441 (1969).
[14]V. Franco, Phys. Rev. 175, 1376 (1968).
[15]D. J. Ernst, J. T. Londergan, Gerald A. Miller, and R. M. Thaler, Phys. Rev. C 16, 537 (1977).
[16]E. Siciliano and R. M. Thaler, Phys. Rev. C 16, 1322 (1977).
[17]L. D. Ludeking and J. P. Vary, Phys. Rev. C 20, 2188 (1979).
[18]K. L. Kowalski, Ann. Phys. (N.Y.) 120, 328 (1979).
[19]N. Austern, in *Selected Topics in Nuclear Theory,* edited by F. Janouch (IAEA, Vienna, 1963).
[20]S. K. Penny and G. R. Satchler, Nucl. Phys. 53, 145 (1964).
[21]M. Gell-Mann and M. L. Goldberger, Phys. Rev. 91, 398 (1953).
[22]L. D. Ludeking, Ph.D. thesis, Iowa State University, 1979 (unpublished).
[23]B. A. Lippmann, Phys. Rev. 102, 264 (1956).
[24]S. D. Baker, R. Bertini, R. Beurtey, F. Brochard, G. Bruge, H. Catz, A. Chaumeaux, G. Cuijanovich, J. M. Durand, J. C. Faiure, J. M. Fontaine, D. Garreta, F.

Hibou, D. Legrand, J. C. Lugol, J. Saudinos, and J. Thirion, Phys. Lett. B52, 57 (1974).
[25]J. K. Dickens, R. M. Drisko, F. G. Perry, and G. R. Satchler, Phys. Lett. 15, 337 (1965).
[26]Gy. Bencze and J. Zimanyi, Phys. Lett. 9, 246 (1964).
[27]T. S. Towner, Nucl. Phys. A93, 145 (1967).
[28]G. R. Smith, Ph.D. thesis, University of Colorado Report LA-8166-T, 1980.
[29]E. Rost and J. R. Shepard, Phys. Lett. B59, 413 (1975).
[30]D. W. Miller *et al.*, Phys. Rev. C 20, 2008 (1979).
[31]A. Boudard *et al.*, Phys. Rev. Lett. 46, 218 (1981).
[32]J. R. Shepard *et al.*, Colorado Annual Report, 1980 (unpublished), p. 123.
[33]J. J. Kraushaar *et al.*, Colorado Annual Report, 1980 (unpublished), p. 127.
[34]D. A. Hutcheon, Proceedings of Los Alamos Workshop on Nuclear Structure with Intermediate Energy Probes, Los Alamos National Laboratory Report LA-8303-C, 1980.
[35]G. Delic and B. A. Robson, Nucl. Phys. A156, 97 (1970).
[36]R. C. Johnson, F. D. Santos, R. C. Brown, A. A. Debenham, G. W. Greenlees, J. A. R. Griffith, O. Karban, D. C. Kocher, and S. Roman, Nucl. Phys. A208, 221 (1973).
[37]G. Molière, Z. Naturforsch. 2a, 133 (1947).
[38]L. I. Schiff, Phys. Rev. 103, 443 (1956).
[39]B. J. B. Crowley and B. Buck (unpublished).
[40]W. Czyz and W. Maximon, Ann. Phys. (N.Y.) 52, 59 (1969).
[41]G. J. Igo, in *High Energy Physics and Nuclear Structure—1975 (Sante Fe and Los Alamos),* Proceedings of the Sixth International Conference on High Energy Physics and Nuclear Structure, AIP Conf. Proc. No. 26, edited by D. E. Nagle and A. S. Goldhaber (AIP, New York, 1975).
[42]A. Chaumeaux, V. Layly, and R. Schaeffer, Ann. Phys. (N.Y.) 116, 247 (1978).
[43]A. Tekou (unpublished).
[44]M. Abramowitz and I. A. Stegun, *Handbook of Mathematical Functions,* National Bureau of Standards Applied Mathematics Series 55 (U.S. Government Printing Office, Washington, D. C., 1968).
[45]J. P. Vary and C. B. Dover, Microscopic Models for Heavy Ion Scattering at Low, Intermediate, and High Energies, Proceedings of the Second High Energy Heavy Ion Summer Study, Berkeley, 1974, Lawrence Berkeley National Laboratory Report LBL-3675, 1974.
[46]D. Vautherin and D. M. Brink, Phys Rev. C 5, 626 (1972). We gratefully acknowledge receipt of the DDHF code from John Negele.
[47]A. Boudard *et al.*, Phys. Rev. Lett. 46, 218 (1981); J. R. Shephard and E. Rost, *ibid.* 46, 1544 (1981); M. Dillig, *ibid.* 47, 147 (1981).
[48]R. V. Reid, Ann. Phys. (N.Y.) 50, 411 (1968).